Aus der Klinik für Innere Medizin III
Hämatologie, Onkologie und Transfusionsmedizin
der Medizinischen Fakultät Charité-Universitätsmedizin Berlin

DISSERTATION

Mutational Analysis in Patients with Uveal Melanomas

zur Erlangung des akademischen Grades
Doctor medicinae (Dr. med.)

vorgelegt der Medizinischen Fakultät
Charité-Universitätsmedizin Berlin

von

Yuehua Mai
aus: Guangdong, China

Datum der Promotion: 27.02.2015

CONTENTS

ABSTRACT

Background: Uveal melanoma (UM) is the most common intraocular tumor that has a strong propensity for fatal metastasis. Extra-ocular extension, recurrence, and metastasis are associated with extremely poor prognosis. There is no standard treatment for the advanced and metastatic disease so far. Genotypic characterization of UM might identify patients who could benefit from a drug-target based approach. Recent studies showed mutations of guanine nucleotide-binding protein G (q) alpha subunits, encoded by *GNAQ* and *GNA11*, are common and they represent an early or initiating event of the malignant transformation [1]. van Raamsdonk [2][3] reported that *GNAQ* and *GNA11* are dominant acting oncogenes. Up to 85% of UMs were found to bear either *GNAQ* or *GNA11* mutations [2][3].

Uveal and cutaneous melanocytes have a similar embryological origin in the neural crest, but their malignant counterpart displays different biological behaviors. UMs metastasize by hematogenous routes because of the high degree of vascularization but absence of draining lymphatics, whereas cutaneous melanomas often spread to regional lymph nodes first. *BRAF* and RAS mutations are often mutated in cutaneous melanomas and both mutations stimulate the MAPK pathway [4]. Most UMs show a constitutive activation of the MAPK pathway, but mutations in *BRAF* and *NRAS* are rare [5][6]. *KIT* can be specifically mutated in acral and mucosal melanoma [7], whereas findings in UM are conflicting [8].

Method: 165 primary UM and 6 matched metastatic specimens were evaluated, quantitative real-time PCR and melting curve analysis were performed to detect mutations in *GNAQ* and *GNA11* codons 183 and 209, *BRAF* codons 597-603, *NRAS* codons 12 and 62, and *KIT* codons 569, 572, 573, 590 and 804. Statistical analysis was carried out to evaluate correlation between mutational status and clinico-pathological parameters.

Results: 24.8% of primary UM specimens had mutations at codon 183 of *GNAQ* and 30% at codon 209. At codon 209 of *GNA11,* 65.2% of the samples were mutated. Mutations in *BRAF*, *NRAS* and *KIT* were comparatively rare. A novel encoding *BRAF* mutation at codon 603 was found. No correlations were observed between mutational status and clinico-pathological prognostic parameters. In the analysis of matched primary-metastatic samples, 3 patients clearly showed mutations only in

metastasis, with one patient acquiring mutations in three different genes.
Conclusion: 85.5% of primary UMs showed mutations either in *GNAQ* or *GNA11*. No association was found between mutational status and prognostic parameters. *GNAQ* or *GNA11* mutations are common also in metastases, but further mutations can be acquired suggestive of cancer clonal evolution.

ABSTRAKT

Hintergrund: Das Aderhautmelanom ist der häufigste intraokulare Tumore und weißt eine starke Metastasierungsneigung auf. Das Auftreten von extraokulärem Wachstum, Rezidiven oder Metastasen ist mit einer schlechteren Prognose assoziiert. Derzeit gibt es keine Standard-Behandlung für das metastasierte uveale Melanom. Die Genotypisierung von UMs könnte eine Identifizierung von Patienten ermöglichen, die von einer zielgerichteten Therapie profitieren könnten. Jüngste Studien zeigten, dass Mutationen von Guanin-Nukleotid-bindendes Protein G (q) alpha-Untereinheiten, codiert durch *GNAQ* und *GNA11*, häufig sind. Sie stellen einen frühes oder auslösendes Ereignis der malignen Transformation dar [1]. *GNAQ* und *GNA11* sind dominant wirkende Onkogene [2][3]. Insgesamt können in bis zu 85% der UMs entweder *GNAQ* oder *GNA11* Mutationen nachgewiesen werden [2][3].

Uveale und kutane Melanozyten haben einen ähnlichen embryonalen Ursprung in der Neuralleiste, aber ihre malignen Equivalente zeigen unterschiedliche biologische Verhaltensweisen. UMs metastasieren insbesondere hämatogene aufgrund der ausgeprägten vaskulären Anbindung, während kutane Melanomen vorrangig lymphogen metastasieren. Bei kutanen Melanomen finden sich gehäuft *BRAF* und *RAS*-Mutationen, welche den MAPK-Weg stimulieren [4]. Die meisten UMs zeigen eine konstitutive Aktivierung des MAPK-Weges, aber Mutationen in *BRAF* und *NRAS* finden sich nur selten [5][6]. KIT Mutationen finden sich insbesondere in akralen und Schleimhaut-Melanom[7], während die Erkenntnisse im UM noch widersprüchliche sind [8].

Methode: 165 primäre UM und 6 korespondierende Metastasen wurden ausgewertet. Es wurde quantitative real-time PCR und Schmelzkurven-Analysen durchgeführt. Es konnten Mutationen in GNAQ und GNA11 Codons 183 und 209, BRAF Codons 597-603, NRAS Codon 12 und 62 und KIT Codons 569, 572, 573, 590 und 804 detektiert werden. Statistische Analysen zur Korrelation des Mutations-Status und der klinischen Parameter wurden durchgeführt.

Ergebnisse: 24,8% der primären UM Proben hatten Mutationen im Codon 183 von GNAQ und 30% in Codon 209. In Codon 209 von GNA11 waren 65,2% der Proben mutiert. Mutationen in BRAF, NRAS und KIT waren vergleichsweise selten. Eine neue BRAF-Mutation in Codon 603 wurde gefunden. Es konnte keine Korrelationen

bezüglich des Mutations-Status und der klinisch-prognostische Parameter beobachtet werde. In der Analyse der primären UM und der korrespondierenden Metastasen wiesen die Proben von 3 Patienten Mutationen nur in der Metastastase auf. Ein Patient erwarb Mutationen in drei verschiedenen Genen.

Fazit: Insgesamt konnten in bis zu 85,5% der primären UMs entweder GNAQ oder GNA11 Mutationen nachgewiesen werden. Es konnte kein Zusammenhang zwischendem Mutationsstatus und prognostischen Parametern gefunden werden. GNAQ oder GNA11 Mutationen sind häufig in Metastasen nachweisbar, aber weitere Mutationen können erworben werden was eine klonale Evolution des Melanoms vermuten lässt.

1. INTRODUCTION

1. 1 Epidemiology:

Uveal melanomas (UMs) are the most frequent intraocular malignancy of adulthood. The uvea is a pigmented vascular layer which underlies the retina and its pigment epithelium throughout the ocular fundus. It consists of the iris, ciliary body and choroid. The main function of the uvea is to provide oxygen and other nourishment to the highly metabolically demanding retinal photoreceptors. About 3% of UMs occurred in the iris. They differ from melanomas of the choroid and ciliary body in that they are smaller in size and less aggressive. Choroidal melanomas represent over 90% of all UMs. They have strong propensity for distant dissemination and they are therefore associated with poor prognosis.

97.8% of UM occurs in white individuals, followed by Hispanics, Asians and blacks [9]. Among whites, the annual incidence was 6.3-6.9 per million. Among Hispanics and blacks, the incidence is lower (around 0.9 and 0.24/million respectively) [10]. Fair complexion and light irides are considered risk factors for development of UM [11][12][13]. In Nordic countries like Denmark, Norway and Sweden, the incidence is up to 8 per million [14][15], whereas in Spain and southern Italy, the incidence is about 2 per million.

UM is extremely rare in children, in most of the series this malignancy is in fact diagnosed in the sixth decade of life with a median age of 55. According to the literature, the frequency in males and females is nearly equal, with slight predominance of males even if in the age group from 20 to 39 a small predilection for women was observed [9][15].

1. 2 Risk factors:

1. 2. 1 Genetic predisposition

UM usually occurs sporadically without any obvious genetic predisposing factors. Findings in some of the familial patients suggest that there may be a genetic predisposition with a dominant autosomal hereditary transmission.

Silcock was the first to report a case of a mother and her two daughters

affected by UM in 1892. Since then, 51 families had been reported having a predisposition for development of UM [16]. Considering that the incidence of UM in the general population is very low, the possibility of developing UM in a family context is accordingly low and it only accounts for 0.6% of patients [17]. Even though, statistical evidence supported the likelihood of a hereditary predisposition, familial predisposition and kinship should be considered to be a part of the aetiological process in UM. Singh identified 17 kindreds with a first-degree relative affected with primary UM and found the expected number of affected first-degree relatives to be 0.81 (RR = 20.99; 95% CI, 12.2-33.6), with an SE of 0.08 ($P < 0.001$) [17]. However, the majority of the familial cases reported are one- or two-generation families and have only one affected member in addition to the proband, only few contain three or more cases of ocular melanoma and are consistent with the inheritance of an autosomal dominant gene with incomplete penetrance.

Individuals with familial tumor predisposition usually develop UM earlier compared to sporadic UM. Studies showed that the mean age at which UMs was diagnosed in familial and sporadic UMs were 42 and 56 years respectively [18]. In addition, inherited susceptibility genes tend to increase the risk of developing multiple cancers at different sites. Relatives of the UM patients have a higher risk of developing other malignancies than ocular cancers, which might reflect the pleiotropic effects of an inherited predisposition. Sing et al. evaluated 27 UM families and found that the risk of developing a second primary tumor was 4-fold higher. Breast, prostate, and cutaneous melanoma were the most common familial malignancies. A follow-up study of 32251 women with ovarian cancer showed the risk of ocular melanoma was increased 4-fold. An increased risk of cutaneous melanoma and ocular melanoma has also been observed in a systematic study of 18010 breast cancer patients [19][20]. Ocular melanocytosis, neurofibromatosis type I, familial atypical mole and melanoma syndrome can also predispose to UM [17].

Several genes have been suggested as possible candidates in hereditary UM including CDKN2A, BRCA2, BAP1 and p14/ARF [21][22]. A high frequency (47.4%) of somatic mutations in BAP1 in primary UM [23] proved to be strongly associated with early development of metastatic disease (class 2 tumors) and seen more commonly in UM with monosomy 3. However, the frequency of germline mutations in these known candidate genes is extremely low, suggesting that the existence of other

additional genes is responsible for hereditary cancer predisposition in UM.

1. 2. 2 Ocular nevi

Clinical and histopathologic evidence showed that melanomas can arise from pre-existing benign ocular nevi. The prevalence of choroidal nevi transforming into malignant melanoma was estimated to be 1 in 8845 annually in the white population [24]. Shields [25] reviewed 2514 consecutive archives of choroidal nevi and identified several factors predicting malignant transformation, including greater thickness, subretinal fluid, symptoms, orange pigment, margin near disc, ultrasonographic hollowness and absence of halo. In teenagers, choroidal nevi tend to appear as a brown stable mass with chronic overlying drusen. In a large population-based series, nevi were present in 6.5% of individuals aged 49 to 97 years. On 42% of nevi clearly visible drusen were seen. They were larger and more centrally distributed as nevi size increased. Nevi were significantly less frequent in individuals with blond hair [26].

1. 2. 3 Melanocytosis

Ocular melanocytosis (OM) is a congenital hyperpigmentation condition of the episclera and uvea, caused by an increased number of fusiform dendritic melanocytes and considered to be the most important etiology factor for UM. In the eyes of vertebrates, the melanocytes have two different embryonic origins: the epithelial retinal cells arise from the neural ectoderm, whereas the uveal melanocytes originate from the neural crest [neural crest-derived melanocytes (NC-Ms)]. When the melanocytes of neural crest cell origin fail to reach the intended surface positions, ocular melanocytosis present [27]. When this condition involves the skin in the distribution of the ophthalmic branch of the trigeminal nerve, it is referred to as oculodermal melanocytosis (ODM, also known as nevus of Ota). The OM/ODM is slightly more common in Asians [28]: the prevalence rate is 0.038% in whites, 0.014% in blacks, and 0.4-0.84% in Asians [29]. However, OM/ODM increasing the risk of UM is much higher in Caucasians [30][31].

1. 2. 4 Hormonal influences

Melanoma cells have estrogen receptors [32][33], and hormonal influences are considered to have a possible association with cutaneous melanoma [34]. Pregnancy may be in fact associated with an increased risk of melanoma through a rapid increase of melanocyte-stimulating hormone (MSH) during early pregnancy. MSH stimulates the cell division of melanocytes and therefore may also promote growth of pre-malignant cells. An early case-control study indicated that women with increased hormone levels had higher risks for UM when compared to women with low hormonal exposures [35]. Contradicting this, some studies observed a decreased risk of UM with increasing amount of pregnancies and no effect of menopausal hormonal therapy or bilateral oophorectomy [36]. Scientists considered that hormonal factors play only a limited role in causing melanomas of the eye [37].

1. 2. 5 Light colored iris

Many studies supported that individuals with light irises are at increased risk of developing UM. Similarly the risk of metastatic death from choroidal melanoma was also increased in patients with light colored iris than in those with dark irises [38][39]. Individuals with blue or gray eyes were shown to have a higher risk with a relative risk of 1.75 (95% CI: 1.31-2.34) as compared with individuals with brown eyes [40].

The protective influence of pigment may be particularly important in the iris, since the iris is an effective ultraviolet filter located in front of the lens, where the sunlight exposure is greatest, and the quantity of uveal melanin in eyes with dark-colored irides is greater than that in light-colored eyes [41][42]. Uveal melanocytes contain both eumelanin and pheomelanin, cells from melanocytes of dark-colored irises have a higher quantity of melanin, and the ratio of eumelanin/pheomelanin is significantly greater than that in light-colored eyes, which therefore can resist reactive oxygen species (ROS) and the malignant transformation of uveal melanocytes [42][43][44].

1. 2. 6 Sunlight exposure

According to biologic effects, the UV region can be further subdivided into UVA (320-400 nm), UVB (280-315 nm) and UVC (100-280 nm). Ultraviolet B (UVB) radiation is carcinogenic and certainly a main cause of skin cancers, most likely cutaneous melanoma [45][46][47]. But, in the uvea tract not all wave lengths of the light can reach the melanocytes in the eye. For iridal melanocytes which are located behind the cornea and anterior chamber, the cornea is transparent to visible light, but it absorbs all the UVC, part of UVB (22-73% at 320-300 nm) and a very small amount of UVA (6-20% at 400-330 nm) [48]. Therefore, in vivo the iridal melanocytes are exposed to visible light, UVA and some of the UVB spectrum. The ciliary body and choroidal melanocytes are covered internally by the retina and densely pigmented ciliary and retinal pigment epithelia and externally by thick and nontransparent sclera. Only 0.1% UVA can pass a juvenile lens [49], in infancy and in early childhood, there is a window of transmission of nearly 8% of UV radiation around 320 nm through the lens, and about 30% of the transmitted UV is absorbed by the retinal pigment epithelium (RPE) before impinging upon the uveal melanocytes [50]. As a result of the transmission properties of the cornea and lens, only visible light reaches the RPE in the adult human eye. Thus, only small fluencies of UV can probably reach the melanocytes in the ciliary body and choroidal.

Sunlight exposure is considered to implicate in the development of iris melanomas. Firstly, iris melanocytes are located in the anterior surface, where they are exposed to the sun radiation. Secondly, the iris melanoma tends to occur in the inferior sector, where exposure to sunlight is greatest [51]. But unlike iris melanoma, the expose of posterior regions to light is very limited, epidemiology studies found choroidal melanomas not distributed a positive correlation with UV [52][53].

Yu reported that solar radiation caused a decrease in the incidence of choroidal melanoma [54]. It is consistent with other reports suggesting that solar radiation reduces the risk and/or mortality of various systemic malignant tumors, such as non-Hodgkin's lymphoma, and prostate, breast, colon and ovarian cancers. This beneficial effect of UV radiation increases the 1.25-dehydroxyvitamin D3, which inhibits growth and induces apoptosis in various malignant tumor cells. Cutaneous and conjunctival melanoctytes are mainly exposed to solar radiation, in these tumors

the direct effect of UV radiation predominates and increases the tumor incidence with decreasing latitude. Uveal melanocytes, consisted with iris, choroidal and ciliary body melanocytes, the iris melanocytes exposed to solar radiation and iris melanoma is UV radiation-related, whereas the choroidal and ciliary body melanocytes are not directly exposed to solar radiation and the indirect protective effect of solar radiation causes a decrease in prevalence.

These researches are interesting hypothesis. However, as these findings have not been confirmed or validated, this hypothesis remains to be proved. In the other hand, the lower incidence of iris melanoma in dark-colored eyes can be explained by the photo-screening effect produced by their more abundant iridal eumelanin [55].

1. 3 Molecular pathogenesis

The development of UM has been associated with early oncogenic mutations, which affect the molecular pathways involved in the regulation of the cell cycle or the control of cell apoptosis. Activation of MAPK pathway is a common event both in cutaneous and uveal melanomas. Unlike cutaneous melanoma, UM generally lacks *BRAF* and *NRAS* mutations. Recent genetic analyses have highlighted the *GNAQ* and *GNA11* mutations, which are early oncogenetic events that activate the downstream cellular pathways.

1. 3. 1 GNAQ/GNA11 and MAP-kinase pathway

83% of UMs carried activating mutations in either *GNAQ* or *GNA11*, but in 282 extraocular melanomas only one had a *GNAQ* mutation [2][3][56]. Lamba et al. analyzed *GNAQ* Q209 mutations in 922 human neoplasms with various histopathological features (no UMs), the only *GNAQ* mutation was found in blue nevi [57]. In van Raamsdonk's study, 45% of UMs harbored *GNAQ Q209* mutations whereas 32% showed *GNA11 Q209* mutations with wild-type *GNAQ*. Mutations were present in all stages of progression [1][5] and there was no correlated with chromosomal aberrations or other clinical features indicative of poor outcome, suggesting that these mutations occur early in tumorigenesis and act as dominant oncogenes [1][58].

Under normal conditions, G-proteins are activated by G-protein–coupled receptors and mediate multiple downstream effectors. Mutations in codon 209 in the ras-like domains of *GNAQ* and *GNA11* resulted in constitutive activation of the Gαq and Gα11 subunits by abrogating their intrinsic GTPase activity required to return them to an inactive state, leading to constitutive activation of the MAPK/ ERK pathway.

The mitogen-activated protein kinases (MAPKs) are conserved proteins that regulate cell growth, division and death. The MAPK pathway represents a cascade of phosphorylation events including three pivotal kinases, namely Raf, MEK (MAP kinase kinase), and ERK (MAP kinase). Activation of this pathway in cutaneous melanocytes has been shown to occur by a variety of mechanisms, including autocrine growth factor stimulation and mutation of the NRAS or BRAF genes. In the active GTP-bound state, RAS activates a number of downstream signaling cascades involved in controlling cell growth and behavior. RAS initially interacts with and activates the serine/threonine protein kinase BRAF that acts in the MAPK pathway to transduce regulatory signals from RAS to mitogen-activated protein kinase/extracellular signal-related kinase (MEK1/2). The signal transducer MEK1/2 phosphorylates extracellular signal-regulated kinase (ERK1/2), leading to the activation of these kinases, which in turn activate a variety of transcription factors, including ELK1, again through phosphorylation [59] [60] (**Figure 1**)

Around 60% of all melanomas have a *BRAF* mutation, and 90% of them are V600E substitution [61]. Activation of the MAPK pathway is involved in mutations in *BRAF* and *NRAS* in cutaneous melanomas, but in UM was not the same case [1][62], activation of the MAPK pathway appears to be induced through *GNAQ*/*GNA11*-mutation which lead G-protein signaling, and ERK as a downstream kinase in the pathway, manifested the activation [63][64].

1. 3. 2 PI3K pathway-PI3K/AKT/PTEN/mTOR

The type I phosphatidylinositol-3-kinase (PI3K)-AKT pathway is initiated at the cell membrane by growth factors interacting with tyrosine kinase as well as G protein-coupled receptors. Phosphorylated AKT (pAKT) can block apoptosis, regulate the actin cytoskeleton and transcription-factor pathways through the Rac and Rho family of proteins. AKT3 gene is found in about 60% of melanomas, and

correlates with melanoma progression [65]. Gene PTEN is a tumor suppressor inhibiting melanoma cell growth by increasing susceptibility of cells to apoptosis [66]. The deletion or silencing of *PTEN* increases the level of AKT3 phosphorylation in melanocytes and early-stage melanoma cells [67]. Recent studies indicated that *PTEN* is involved in the *PI3K* pathway as negative regulator of *AKT*. Loss of function of *PTEN* by deletion or mutation, leads to activation of *AKT* and over-expression of the *PI3K-PTEN-AKT* pathway preventing apoptosis [68][69]. Inactivation of *PTEN* is reported in 15% of UM cases and has been linked to an increase in aneuploidy but also poor clinical outcome [68]. This may suggest a role in later stages of tumor growth and development. Activating mutations of *AKT3* may also lead to activation of this pathway, though mutations of *AKT3* have not been reported in UM up till now. The mammalian target of rapamycin (mTOR) lies downstream of *AKT* and can regulate its activity by feedback mechanisms. *mTOR* forms at least 2 active complexes of proteins: mTOR1 and Mtor2, the first of which suppresses and the second activates *AKT* signaling. (**Figure 1**)

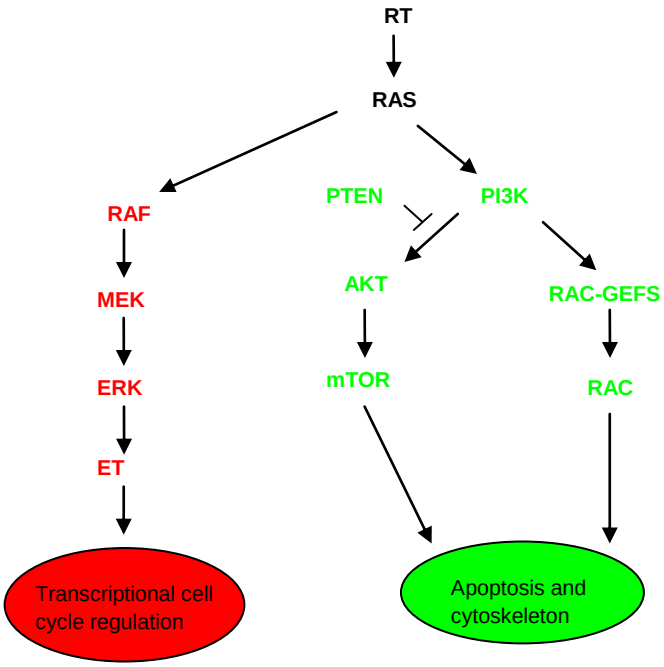

Figure 1. The main effectors of RAS signaling. (Figure originated from Anton Platz et al., 2008 and Philip Friedlander et al., 2010.)

1. 3. 3 KIT

c-KIT belongs to the Type III tyrosine kinase receptor family. The ligand for c-KIT is the stem cell factor (SCF) and the SCF-KIT pathway regulates the differentiation of melanocytes, red blood cells, mast cells, interstitial cells of Cajal, and germ cells. Moreover, this pathway is important in the survival of primordial germ cells. Expression of c-KIT and gain-of-function mutations in c-KIT has been found in mastocytosis, leukemia and gastro-intestinal stromal tumors.

KIT binding of its ligand, stem cell factor (SCF), resulting in activation of downstream signaling pathways including the MAPK pathway and the PI3K/AKT pathway (**Figure 2**). These pathways play a critical role in the development of melanocytes/normal uveal melanocytes [70]. Loss-of-function alleles lead to defects in melanocyte migration, survival, proliferation and differentiation. The prevalence of *KIT* mutations varies between melanoma subtypes, which were observed in 17% of melanomas on chronically sun-damaged skin, 11% of melanomas on acral surfaces, 21% of melanomas on mucosal surfaces, but less than 1% of melanomas on intermittently sun-exposed skin [7], while the last subtype is often characterized by *BRAF* and *NRAS* [71]. Ocular melanomas have been reported to express *KIT* at frequencies between 63 and 91%, but findings for *KIT* mutations in ocular melanoma are conflicting. Some reports showed *KIT* mutation frequency to be less than 1% [72] [73]. In contrast, Wallander et al. found 9% of their series showed *KIT* mutation in their study, which suggested that *KIT* mutations occur in melanomas derived from all ocular anatomical locations [74].

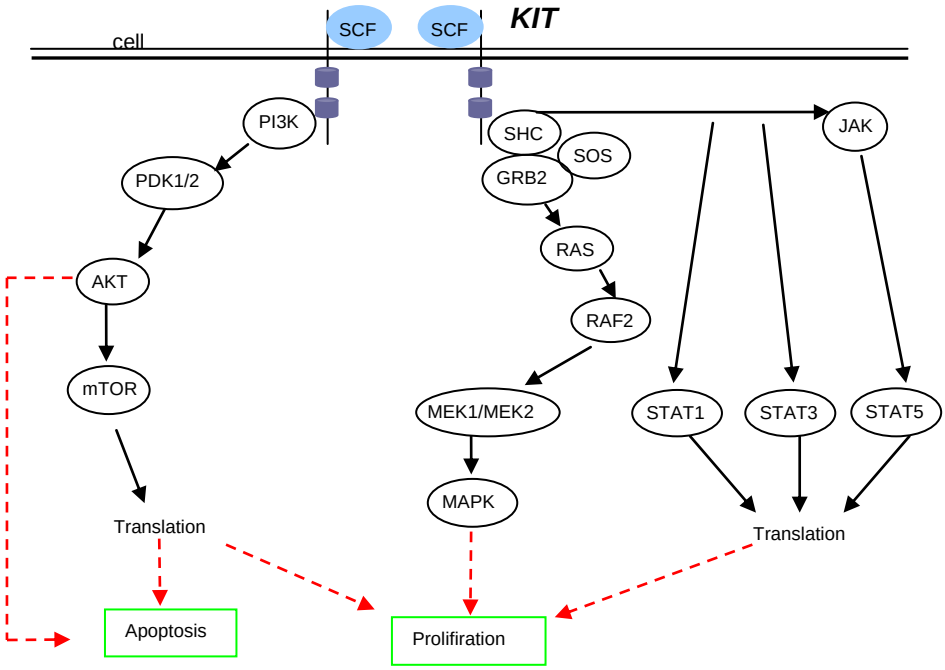

Figure 2. KIT signal transduction. (Figure originated from Anette Duensing)

1. 4 Pathology and prognosis

UMs are classified as spindle A cells, spindle B cells, epithelioid cells and intermediate cells according to Callender classification (Modified by McLean et al. 1978). Spindle A cells are spindle-shaped cells with slender nuclei and lacking visible nucleoli, while spindle B cells are plumper and more oval in shape and have coarser chromatin and distinct nucleoli. UM patients composed of spindle A cell-type have a 5-year survival rate of approximately 95% compared with an 84%-89% survival rate for spindle B cell-type patients. Epithelioid cells have abundant cytoplasm and are often polygonal in shape. They have distinct cytoplasmic margins, are poorly cohesive, and do not grow as a syncytium. The nuclei of epithelioid cells typically are round or oval in shape, and they often appear vesicular due to margination or clumping of chromatin along the inner side of the nuclear membrane. Epithelioid melanoma cells also have prominent nucleoli that are often large and reddish purple in color. UMs that contain epithelioid cells have a poorer prognosis. The 5-year survival rate for UM patients with epithelioid cell type ranges

from 30% to 43%. The mixed cell type combined spindle and epithelioid cells and have a 40% to 50% 5-year survival rate. The prognosis proportionately worsens as the percentage of epithelioid cells increases. However, pure epithelioid-cell primary melanomas are rare, accounting for approximately 3% of cases [75]. In the Collaborative Ocular Melanoma Study, mixed-cell type melanomas represented the predominant pattern, accounting for the 86% of cases.

Up to 50% of patients with primary UM will ultimately develop distant metastasis. The most common site of metastasis is the liver (90%), then the lung (30%), the bone (23%) and the skin (17%) [76]. Patients with only extrahepatic metastases have significantly longer survival (median, 19-28 months) compared to those with liver metastasis. The Collaborative Ocular Melanoma Study (COMS) identified 5- and 10-year cumulative metastasis rates of 24% (95% CI, 23% to 26%) and 32% (95% CI, 30% to 34%), respectively [77]. Patients are at risk to develop metastasis up to 20 years after the initial diagnosis.

There are several important indicators predicting metastatic disease, they are basal tumor diameter, ciliary body involvement, transscleral extension, epithelioid melanoma cytomorphology, high mitotic rate, extravascular matrix pattern such as closed loops, microvascular density, chromosomal abnormalities, and class 2 gene expression [78][79]. Damato and others identified tumor size and basal tumor diameter as the most important independent predictors [80][81][82]. Monosomy 3 which is found in 50-60% of primary tumors confers higher aggressiveness and poorer clinical prognosis [83]. Other chromosomal aberrations include gain in chromosomal 8 and loss of chromosomal arm 1p also predict poor prognosis, concurrent loss of 1q and chromosome 3 predict a shorter survival [84] [85]. A study of 220 posterior melanomas showed monosomy 3 (Hazard ratio [HR] 2.83, P = 0.002) and gain of chromosome 8q (HR 3.13, P = 0.002) as the most important independent prognostic factors of poor survival, followed by older patient age (HR 1.02, P = 0.017) [86].

The 5-year mortality rate of UM patients has not changed significantly since 1973 [87]. The survival rates at 5, 10, and 15 years are 65%, 52%, and 46%, respectively [88][89]. The median survival for a hepatic metastasis is 6 months with an estimated survival of 15-20% at 1 year and 10% at 2 years, irrespective of treatment[76][90].

1. 5 Diagnosis

Approximately 30% of ocular melanoma patients have no symptoms at time of diagnosis [91], patients may be diagnosed after developing symptoms of blurred vision, a dark spot on the eyelid or iris, or a change in the pupil's shape. In some cases, iris melanoma occurs in the inferior portion of the iris and produces tumor seeding onto the stroma and into the anterior chamber angle, which would cause the melanoma cells and debris shedding into the trabecular meshwork that obstructs aqueous outflow, leading to elevated intraocular pressure (secondary glaucoma). Many posterior melanomas are discovered by routine eye examination. Modern diagnostic techniques such as slit lamp biomicroscopy, indirect ophthalmoscope (IO), ultrasonograph, fundus fluorescein angiography (FFA), and transillumination are also applied. Fine needle aspiration cytology (FNAC) should only be considered if therapeutic intervention is indicated and diagnosis cannot be established by any other means.

The diagnosis of metastases is routinely made through regular screening test like measurement of liver function tests, liver ultrasound, computed tomography scan or MRI. There is some evidence that MRI is superior to detect small metastases rather than FDG-PET [92][93]. The best screening tests to detect early recurrence remains to be prospectively determined, preferably in the context of follow-up after an adjuvant therapy.

1. 6 Treatment

1. 6. 1 Local treatment

There are several options available for primary UM, from primary enucleation to local resection, laser photocoagulation, and, most commonly, eye and vision sparing radiation therapy, depending on visual acuity of the affected eye, visual acuity of the contralateral eye, tumor size, location, ocular structures and presence of metastases.

Enucleation is typically performed for advanced melanomas that occupy most of the intraocular space or cause severe secondary glaucoma. It is also indicated for primary tumours that have invaded the optic nerve or have extraocular extension.

Local resection comprises the trans-scleral tumor resection (TSR) and endoresection. TSR can be lamellar or full thickness, and the partial thickness techniques have been more commonly employed. Partial thickness resection requires dissection of a lamellar scleral flap. Ocular decompression by limited pars plana vitrectomy, resection of the tumor together with the deep scleral lamella, and closure of the eye by suturing of the lamellar scleral flap. Due to initially high tumor recurrence rates, adjunctive radiotherapy has been added before or after TSR. However, the poor local control rates, coupled with a high incidence of post-operative complications (secondary rhegmatogenous retinal detachment, intraocular hemorrhage, ocular hypotony, and phthisis) and concerns about UM's dissemination, have limited the widespread use of TSR. Endoresection is typically indicated after radiation therapy. Surgery is performed with a vitrector through a retinotomy or beneath a retinal flap. An air–fluid exchange drains residual subretinal fluid; endolaser photocoagulation is used to destroy any residual intrascleral tumor and to achieve retinopexy. Silicone oil is typically required. Although endoresection aims to reduce tumor-related ocular morbidity, it increases known risks of vitreoretinal complications [94].

Plaque brachytherapy and proton beam radiotherapy have developed to be the most common ocular treatment. Such conservative therapy shows a similar survival rate and metastasis risk as enucleation, with the advantage of better cosmetic results and the possibility of saving vision [95]. The original cobalt-60-based plaques, which produced high-energy gamma rays with greater irradiation of normal structures, the patient, and the surgeon, were now replaced by lower-energy ruthenium-106, iodine-125, and palladium-103 sources [96][97]. Transpupillary thermotherapy (TTT) can be performed in order to treat small and pigmented melanomas; tumor resection may be indicated in small iris and ciliary body melanomas.

1. 6. 2 Therapy for the metastatic disease

Because liver metastasis occurs in up to 90% of the cases and has poorer prognosis, efforts have been made to develop loco-regional management of liver metastases. Options include surgery, radio-frequency ablation for solitary small lesions, hepatic intra-arterial chemotherapy, immuno-embolization and transarterial

chemo-embolization (TACE) and hepatic arterial perfusion.

Hepatic intra-arterial chemotherapy is based on the use of an implantable hepatic catheter and a drug, such as fotemustine, that has high systemic clearance and a high extraction rate allowing maximum local exposure. Becker reported a series of patients with hepatic metastasis treated with fotemustine, IFN and IL-2 infusion into the hepatic artery and a group of patients with extrahepatic disease treated with i.v. fotemustine. Objective responses were 22% and 8% respectively, but a similar median survival was observed [98]. Peters [99] evaluated intrahepatic infusion of 100 mg/m^2 fotemustine in 101 patients with metastatic uveal melanoma and liver metastasis. 15 patients had a radiologic complete response (CR), 21 achieved a partial response (PR) and 48 had stable disease (SD); the overall objective response rate of 36% and overall survival was 14 months. It led to a randomized phase III study (EORTC18021) comparing hepatic intra-arterial versus intravenous fotemustine in patients with liver metastasis only. 171 patients were randomized (HIA: 86, IV: 85). Due to poor accrual, an interim analysis was performed after 134 deaths in order to test futility (power=79%). In May 2011, the hazard ratio for OS, HR = 1.097, was greater than the critical value, HR = 0.87. The Independent Data Monitoring Committee recommended stopping accrual for futility. In January 2012, treatment comparison provided similar results. HIA fotemustine led to a higher ORR (12% versus 2%) and longer PFS (HR=0.62; 6-month rate 41% versus 27%; 1-year rate: 19% versus 8%) compared to IV administration. HIA did not translate into an improvement in OS (median ~ 13.5 months).

Immuno-embolization is a novel approach for transarterial embolization of hepatic metastases: the chemotherapy agent is replaced by an immunologic stimulant (GM-CSF), with the objective of destroying cells by the ischemic effects of embolization, stimulating antigen-presenting cells, facilitating antigen uptake and enhancing systemic immunity against tumor cells. A phase I clinical trial was conducted in 39 patients with malignant hepatic tumors, including 34 UMs: among 31 evaluable patients, 2 complete responses (CR), 8 partial responses (PR) and 10 stabilizations of disease (SD) were observed and median overall survival of intent-to-treat patients was 14.4 months. Based on these results, a randomized phase II clinical trial is currently enrolling UM metastatic patients, who will undergo embolization of the hepatic artery with or without 2000 mcg of GM-CSF [100][101].

Isolated hepatic perfusion (IHP) is a treatment that exposes the liver to high doses of chemotherapy to obtain maximal tumor shrinkage but not causing fatal hepatotoxicity. Ongoing clinical trials are evaluating the use of IHP in association with melphalan and temozolomide.

1. 6. 3 Targeted therapies

The new insights in the biology of UMs have attracted great interest in developing innovative therapeutic approaches targeting either the microenvironment or directly the activated intracellular pathways. Drugs designed to interfere with a specific molecular pathway are believed to have a critical role in tumor growth or progression.

Mutations of *GNAQ* and *GNA11* drive inappropriate proliferative signaling from MAPK or PI3K/AKT pathways, but currently small molecules able to antagonize constitutively the activated domain of *GNAQ* are not available yet. Blocking downstream signaling is currently being tested to inhibit MAPK/ERK pathways in a randomized phase II of AZD 6244 versus temozolomide (NTC 01143402). Preliminary results were reported at the International Congress of Ocular Oncology in Buenos Aires in a small number of patients and they were very promising with a 40% response rate with AZD 6244 and 9% with temozolomide. Other potential targets that are currently under investigation as phospholipase C (PLC), which is activated by Gq, and ends up to a RAS-independent signaling mechanism involving protein kinase C(PKC) family-dependent ERK pathway [57]. PKC inhibitors are also under evaluation in a phase II trial (NCT01430416).

The activated pathways, which are induced by the over-expression of receptors like c-*KIT*, c-MET and IGF-1R, are now being tested in series of clinical trials with imatinib. Penel gave a high dose (800 mg/day) of imatinib in 13 patients without any antitumor effect. All patients except one progressed but the median overall survival was 10.8 months [102]. Hofmann gave a dose of 600 mg/day of imatinib to 12 patients with tumor expressing a high level of c-*KIT*. Only one obtained stabilization. The median overall survival was 7.8 months [103]. Although it was established as therapeutic target in other melanoma subtypes, imatinib alone does not achieve a satisfactory solution in this disease.

As with MAPK, PI3K/AKT signaling is initiated at the cell membrane by growth

factors interacting with RTK and G-protein-coupled receptors, drugs that modify the PI3K/AKT pathway are under investigation. The inhibitors of mTOR, temsirolimus and everolimus, have been conducted in renal cell carcinoma and metastatic melanoma, respectively, the influence in UM has not been reported. Several drugs such as RTK and cyclooxygenase (COX) inhibitors target the PI3K/AKT pathway indirectly and cause blockage of AKT phosphorylation and induce apoptosis. Nepafenac is a COX-2 inhibitor used for ocular inflammatory processes and discovered to delay the progression of UM in animal models [104]. Drugs that modify the pathway more directly are being developed.

The addition of antiangiogenic agents to chemotherapy has resulted in improved efficacy of tumor control in a variety of malignancies [105][106]. Vascular endothelial growth factor (VEGF) is an endothelial mitogen that mediates angiogenesis. Down-regulation of VEGF activity in UM xenograft models inhibited tumor cell growth [107]. Sunitinib, a multi-targeted tyrosine kinase inhibitor against VEGFR, FLT-3, c-*KIT*, and platelet derived growth factor receptor (PDGFR) are currently part of a phase II study in combination with temozolomide (NCT 00859326). In a pilot study with 20 pretreated patients, Sunitinib showed an antitumor activity with one partial remission and 12 stabilizations (clinical benefit: 65%). The median PFS and overall survival were 4 and 8.2 months, respectively [108]. Bevacizumab, (Avastin, Genentech) is a monoclonal antibody that blocks angiogenesis by binding to VEGF, preventing coupling to the VEGF receptor. The addition of bevacizumab to carboplatin and paclitaxel in a randomized phase II study of advanced melanoma patients demonstrated an improvement in the primary endpoint of median PFS (5.6 vs. 4.2 months), the overall survival improved with the addition of bevacizumab (12.3 vs. 9.2 months), these trends are not statistically significant, thus further investigation is required to optimize targeted anti-angiogenic therapeutic approaches.

2. AIMS AND SCOPE OF THIS STUDY

UM is the most common intraocular malignancy in Caucasians and no effective treatment is available for the metastatic disease so far. Genotypic characterization of UM might identify patients who could benefit from a drug-target based approach. The present investigation studies the *GNAQ*, *GNA11*, *BRAF*, *NRAS* and *KIT* mutational status in a large series of UM patients and evaluates their possible associations with clinico-pathological prognostic parameters. In order to assess clonal evolution, matched metastatic tissue samples have also been analyzed in 6 selected patients.

3. MATERIAL AND METHODS

3. 1 Materials

3. 1. 1 Uveal melanoma specimens

Formalin-fixed-paraffin-embedded (FFPE) archival biopsy specimens of 165 primary UMs and six selected matched metastasis specimens were randomly selected and retrieved after obtaining approval from the files of the Department of Ophthalmology. All cases were reviewed to confirm the original diagnosis and to ensure that sufficient tumor (> 50% of the entire tissue specimen) was present for analysis.

3. 1. 2 Cell lines in cultured

Cell lines	Origin	Provider
92-1	primary uveal melanoma	Leiden, Netherlands
Mel202	primary uveal melanoma	Leiden, Netherlands
Mel270	primary uveal melanoma	Leiden, Netherlands
OMM2-3	primary uveal melanoma	Leiden, Netherlands
Hela	cervical carcinoma	DSMZ, Heidelberg, Germany
SK-MEL-28	malignant melanoma	ATCC, Rockville, MD, USA
MCF-7	breast adenocarcinoma	DSMZ, Heidelberg, Germany
Molt4	T lymphoblast	DSMZ, Heidelberg, Germany
HL-60	Human lymphoblast	DSMZ, Heidelberg, Germany

3. 1. 3 Cell culture and cell mediums

Name	Manufacturer
PBS	Biochrom AG, Berlin, Germany
RPMI 1640	Biochrom AG, Berlin, Germany
DMEM	Biochrom AG, Berlin, Germany
Eagles MEM	Biochrom AG, Berlin, Germany
Penicillin 10 000 U/ml	Gibco BRL, Karlsruhe, Germany
streptomycin	Gibco BRL, Karlsruhe, Germany
L-Glutamine	Gibco BRL, Karlsruhe, Germany
fetal bovine serum(FBS)	Gibco BRL, Karlsruhe, Germany

3. 1. 4 Genomic DNA extraction solutions and buffers

Reagent	Manufacturer
Ultra-Pure Water	Biochrom, Berlin, Germany
xylene	Carl Roth, Germany
Cell lysis solution	Qiagen, Hilden, Germany
Proteinase K	Qiagen, Hilden, Germany
RNase A solution	Qiagen, Hilden, Germany
Protein precipitation solution	Qiagen, Hilden, Germany
Isopropanol	Merck Schuchardt OHG, Germany
Ethanol	J.T. Baker, Netherlands
DNA Hydration solution	Qiagen, Hilden, Germany

3. 1. 5 Genomic DNA purification solutions and buffers

Name	Manufacturer
DNA Binding Buffer	DNA Clean&Concentrator, Zymo Research, Freiburg, Germany
Wash Buffer	DNA Clean&Concentrator, Zymo Research, Freiburg, Germany
PCR-graded water	Roche, Mannheim, Germany

3. 1. 6 Polymerase chain reaction solutions and buffers

Name	Manufacturer
PCR-graded water	Roche, Mannheim, Germany
Magnesium dichloride 25mM	Roche, Mannheim, Germany
LC-FastStart Enzyme 1a	Roche, Mannheim, Germany
LC-FastStart Enzyme 1b	Roche, Mannheim, Germany
Primers	Metabion, Martinsried, Germany
Probes	Metabion, Martinsried, Germany
Opti Buffer	Bioline, Luckenwalde, Germany
dNTP mix	Roche, Mannheim, Germany
Magnesium dichloride 25mM	Bioline, Luckenwalde, Germany
BSA(Bovine Serum Albumin)	Invitrogen, Karlsruhe, Germany
Taq polymerase BIOX-Act Short	Bioline, Luckenwalde, Germany

3. 1. 7 Other chemicals

Name	Manufacturer
Agarose	Biozym Scientific, Germany
Nucle acid staining solution Red Safe	iNtRON Biotechnology, Germany
DNA loading dye	Fermentas, Germany
TBE	Genaxxon Bioscience, Germany
Gel extraction QX1 buffer	Qiagen, Hilden, Germany
Gel extraction PE buffer	Qiagen, Hilden, Germany
Gel extraction QX2 reagent	Qiagen, Hilden, Germany
TOPO Vector	Qiagen, Hilden, Germany
SOC media	Qiagen, Hilden, Germany
Trypan blue	Qiagen, Hilden, Germany
DMSO	Sigma, Deisenhofen, Germany

3. 1. 8 Laboratory inventory

Product	Name	Manufacturer
Spectrophotometry	Nanodrop 2000	Thermo Scientific, Rockford, IL, USA
Agarose gel chamber	Horzon 58	GibcoBRL, Karlsruhe, Germany
Centrifuge	Eppendorf 5402	Eppendorf, Hamburg, Germany
Incubator	Thermomixer 5436	Eppendorf, Hamburg, Germany
Pipettes	Eppendorf	Eppendorf, Hamburg, Germany
Incubator	Steri-cult2000	Labortect, Goettingen, Germany
Microscope	Zeiss	Zeiss, Goettingen, Germany
Microwave oven	Moulinex	Moulinex, Solingen, Germany
Themoblock	Eppendorf 5436	Eppendorf, Hamburg, Germany
Thermocycler	LightCycler	Roche, Mannheim, Germany
Thermocycler	DNA Engine	BIORAD Laboratories, Munich, Germany
Vortexer	VF2	IKA, Staufen, Germany
Safe bench	Heraeus	Heraeus, Germany
37°C incubator	Heraeus	Heraeus, Germany
Microtome	Leica	Germany

3. 1. 9 Laboratory materials

Material	Manufacturer
Culture flasks	NUNC, Wiesbaden, Germany
Cell scrapers	Sarstedt, Nuembrecht, Germany
Falcon tubes(15 ml and 50 ml)	BDFalcon, Heidelberg, Germany
Tubes (1.5ml and 2 ml)	Sigma, Deisenhofen, Germany
Neubauer chamber	Sigma, Deisenhofen, Germany
Zymo-Spin Column	Zymo Research, Freiburg, Germany
Scalpel	PFM Medical, Cologne, Germany
Microscope slides	SuperFrost, Germany
PCR capillaries	Roche, Mannheim, Germany

3. 2 Methods

3. 2. 1 Cell lines:

Nine cell lines were cultured, they are UM cell lines 92-1, Mel202, Mel270, OMM2.3, cervical carcinoma cell line Hela, malignant melanoma cell line SK-MEL-28, breast adenocarcinoma cell line MCF-7, T lymphoblast cell line Molt 4, and human lymphoblast cell line HL-60. Medium changes and all the other procedures were performed under a clean air bench. The frozen cells were thawed in a water bath at 37°C and dissolved in warm medium. Cells were washed twice in medium to remove DMSO (final concentration < 0.01%) and sowed in flask at the density recommended by the provider. 92-1, Mel202, Mel270, OMM2.3, SK-MEL-28, Molt-4 and HL-60 were cultured in RPMI 1640 medium (Biochrom AG, Berlin, Germany), supplemented with 1% of a stock solution of penicillin/streptomycin, 2% L-glutamine, only the Molt-4 cell line was supplemented with 20% fetal bovine serum (FBS), others with 10% FBS. Hela were cultured in DMEM (Biochrom AG, Berlin, Germany) with 10% FBS, 2% L-Glutamine and 1% penicillin/streptomycin. MCF-7 was cultured in Eagles MEM (Biochrom AG) with 10% FBS, 2% L-Glutamine and 1% penicillin/streptomycin. All cell lines were grown at 37°C, in 5% CO_2 and 95% humidified sterile air. The complete growth medium was renewed twice a week and the cells were harvested at 80% confluence.

Cells were harvested by scraping and medium-washed. Viable cell count was obtained after staining 1:1 with trypan blue by means of Neubauer Chamber. Cells were washed twice by PBS, centrifuged at 1200 rpm for 5 min, and supernatant was discarded. Cell pellet was resuspended with cell lysis solution before genomic DNA extraction.

3. 2. 2 Genomic DNA extraction from microdissected FFPE specimens and cell lines

Genomic DNA was extracted by means of Gentra Pure Core A Kit (Qiagen GmbH, Hilden, Germany). For each FFPE sample, 40mg, 10-µm-thick sections were microdissected, washed in xylene and ethanol and digested with proteinase K. DNA purification was performed after extraction (DNA Clean&Concentrator, Zymo

Research, Freiburg, Germany). Genomic DNA from cultured cells was extracted by Gentra Pure Core A Kit (Qiagen GmbH, Hilden, Germany) following the manufacturer's instructions. DNA concentration was determined by spectrophotometry (Nanodrop 2000, Thermo Scientific, Rockford, IL, USA).

3. 2. 3 Quantitative real time PCR and melting curve analysis

Expression of housekeeping gene HMBS (hydroxymethylbilane synthase, HMBS; also known as porphobilinogen deaminase, PBGD) was measured in duplicate by real-time PCR (Light Cycler software version 3, Roche Diagnostics, Mannheim, Germany) in order to assess the quality of all the sample. HMBS quantification was performed as previously described and only samples with acceptable amount of DNA (HMBS c.p-values ≤ 39) were considered suitable for melting curve mutation analysis.

Primer and probe sequences for *GNAQ*, *GNA11*, *BRAF*, *NRAS* and *KIT* were designed in order to bind the wild-type form of the genes *GNAQ* (codons 183 and 209), *GNA11* (codons 183 and 209), *BRAF* (codon 600), *NRAS* (codons 12 and 61) and *KIT* (codons 569/572/573, 590 and 804) by means of LightCycler Probe Design Software 3.0 (Roche, Mannheim). All the primers and probes were purchased from Metabion (Martinsried, Germany). Sequences are listed in **Table 1**.

Table 1. Primer and probe sets for quantitative and mutational analysis (real time PCR)

Target	Primers/Probe Sequences		Amplicon (bp)
HMBS (NM_000190.3)	Fw:	5'-TGCAGGCTACCATCCATGTCCCTGC-3'	187
	Rev:	5'-AGCTGCCGTGCAACATCCAGGATGT-3'	
	Anchor:	5'-CGTGGAATGTTACGAGCAGTGATGCCTACC-3'	
	Sensor:	5'-LC Red 640-TGTGGGTCATCCTCAGGGCCATCTTC-Pho-3'	
GNAQ codon 183 (NM_002072.3)	Fw:	5'-TTACCAAATGTACTCAAGGCATAAA -3'	222
	Rev:	5'-ACTGACATTCTCATTGTGTCT -3'	
	Anchor:	5'-LC Red 640-TTGCGTAGGCAGGTAGGCAGG-Pho-3'	
	Sensor:	5'-GGGACTCGAACTCTAAGCACATCT-Fluorescein -3	
GNAQ codon 209 (NM_002072.3)	Fw:	5'-CTCATTGTCTGACTCCACG -3'	212
	Rev:	5'-AGTTTGTAAGTAGTGCTATATTTATGTTG-3'	
	Anchor:	5'-LC Red 640-ATGGATACACTGCTTTGAAAATGTCACCTCTATCA-Pho-3'	
	Sensor:	5'-GGGCCAAAGGTCAGAGAGAAGA-Fluorescein -3'	
GNA11 codon 183 (NM_002067.2)	Fw:	5'-TGCAGCTACCTGACCGA-3'	296
	Rev:	5'-ATGAGGTCTGGCTATGTTG-3'	
	Anchor:	5'-LC Red 640-CCACCACCGGCATCATCGAGTAC-Pho-3'	
	Sensor:	5'- CTGCGGGTCCGCGT-Fluorescein-3'	
GNA11 codon 209	Fw:	5'-TGTCAGTCTGGTGTGGCA-3'	219
	Rev:	5'-ACCAGGACTTGGTCGTA-3'	

(NM_002067.2)	Anchor :	5’-LC Red 640-TCCGACCGCTGGCCC-Pho-3’	
	Sensor :	5’- TTCTCAAAGCAGTGGATCCACTTCCTCC-Fluorescein-3’	
BRAF (NT_007914.15)	Fw:	5’-TCAGCAGCATCTCAGGG-3’	199
	Rev:	5’-TTCCTTTACTTACTACACCTCAGATA-3’	
	Anchor :	5’-LC Red 640-AGACCAAAATCACCTATTTTTACTGTGAGGTCTT-Pho-3’	
	Sensor :	5’- CCCACTCCATCGAGATTTCACTGTAG-Fluorescein-3’	
NRAS codon 12 (NT_032977.9)	Fw:	5’-GATCCGACAAGTGAGAGAC-3’	214
	Rev:	5’-CGCCAATTAACCCTGATTAC -3’	
	Anchor :	5’-ATTAGCTGGATTGTCAGTGCGCTTT-Fluorescein-3’	
		Sensor: 5’-LC Red 640-CCAACACCACCTGCTCCAAC-Pho-3’	
NRAS codon 61 (NT_032977.9)	Fw:	5’-TACACAGAGGAAGCCTTCG -3’	213
	Rev:	5’-ATGCTTATTTAACCTTGGCAATAG -3’	
	Anchor :	5’-AACCTGTTTGTTGGACATACTGGATACAGC-Fluorescein -3’	
	Sensor :	5’-LC Red 640-GACAAGAAGAGTACAGTGCCATGAGAG-Pho-3’	
KIT codon569/572/573 (NM_000222.2)	Fw:	5’-TTTGTTCTCTCTCCAGAGTGC-3’	239
	Rev:	5’-GGTGACATGGAAAGCCC -3’	
	Anchor :	5’-LC Red 640-CACAAATGGGAGTTTCCCAGAAACAGG-Pho-3’	
	Sensor :	5’-TATGTTTACATAGACCCAACACAACTTCCTTATG-Fluorescein-3’	
KIT codon 590 (NM_000222.2)	Fw:	5’- CAATTATGTTTACATAGACCCAACACAA -3’	156

	Rev:	5’- GGAAGCCACTGGAGTTC -3’	
	Anchor:	5’-GGTGACATGGAAAGCCCCTGTTTCATAC-Fluorescein -3’	
	Sensor:	5’-LC Red 640-ACCAAAACTCAGCCTGTTTCTGG-Pho -3’	
KIT codon 804 (NM_000222.2)	Fw:	5’-CTTTACAAGTTAAAATGAATTTAAATGGTT -3’	193
	Rev:	5’-GAGAATGGGTACTCACGTTT -3’	
	Anchor:	5’-TCACAGAGACTTGGCAGCCAGAAATATCCTCCTTA-Fluorescein -3’	
	Sensor:	5’-LC Red 640-CATGGTCGGATCACAAAGATTTGTGA-Pho-3’	

Mutational status has been detected by melting curve analysis after quantitative real-time PCR. PCR conditions were optimized and detailed in **Table 2**. For each PCR, two microliters of gDNA were diluted to a volume of 20µl of PCR Mix (LightCycler Faststart DNA Master Hybridization Probes, Roche Diagnostic) containing 0.5 pmol of primer and 0.2 pmol of probe and a final $MgCl_2$ concentration as optimized and listed in the table. Samples were amplified with a pre-cycling hold at 95°C for 10 min, followed by cycles of denaturation at 95°C, annealing and elongation, whose parameters are catalogued and detailed. A final extension at 72°C for 2 min followed the amplification cycles. For determination of analytic mutation, mutational status of cultured cells has to be defined at the very beginning. Internal controls of wild type form and mutated forms from genomic DNA of cultured cells were added to each PCR run. Specimens which showed melting curves not representative of one of the forms of the internal controls, were commercially sequenced (Gene Analysis Service GmbH-Berlin, Germany). Furthermore, a randomly selected number of 18 cases with mutations detected by melting curve analysis were also commercially sequenced for validation. In all cases, mutations suggested by melting curve analysis were confirmed by sequencing.

Table 2. PCR conditions for quantitative and mutational analysis (real time PCR)

Target	$MgCl_2$ concentrations	Cycle	Slope (°C/S)	Annealing (Time and Temperature)	Elongation (Time and Temperature)
HMBS	4mM	45		12 sec, 65 °C	10 sec, 72 °C
GNAQ_183	3mM	50	4	12 sec, 64 °C	8 sec, 72 °C
GNAQ_209	3mM	50	2	12 sec, 64 °C	7 sec, 72 °C
GNA11_183	2mM	50	2	10 sec, 53 °C	9 sec, 72 °C
GNA11_209	2mM	50	2	10 sec, 56 °C	8 sec, 72 °C
BRAF	5mM	50	2	12 sec, 64 °C	8 sec, 72 °C
NRAS_12	3mM	50	2	12 sec, 62 °C	8 sec, 72 °C
NRAS_61	6mM	50	2	10 sec, 67 °C	6 sec, 72 °C
KIT_569/572/573	5mM	50	2	12 sec, 66 °C	9 sec, 72 °C
KIT_590	6mM	50	2	12 sec, 60 °C	6 sec, 72 °C
KIT_804	4mM	50	2	12 sec, 59 °C	7 sec, 72 °C

3. 2. 4 Precautions to minimize technical error

Proper laboratory technique is very important for a successful real-time PCR, which leading to an accurate measurement of melting curve analysis. The following precautions were taken to minimize the potential for cross-contamination between samples and prevent carryover of nucleic acids from one experiment to the next.

Firstly, clean lab coat and clean gloves were needed when preparing samples of PCR amplification. Change gloves whenever they were suspected to be contaminated. Maintain separate areas, dedicated equipment, and supplies for sample preparation and PCR setup. Care must be taken to avoid contaminating the area with plasmids or amplicons, amplified PCR products were not allowed to bring into the designate clean area. Secondly, positive-displacement or air-displacement pipettes were used with filter-plugged tips, pipets must be frequently cleaned with 70% ethanol, and tips were changed after each use. PCR-grade water was used and reagents were dedicated for PCR use only. In addition to taking the above

precautions, a negative control and a positive control should be always included in the PCR assays. To minimize statistical variation in experimental results, sufficient amounts of Master Mix should be prepared for replicate reactions. All samples were processed in triplicate. Repeated freezing and thawing were minimized by preparing small aliquots of stock reagent before first use.

3. 2. 5 Gel electrophoresis

Gel electrophoresis was used to identify the PCR products in this study. During electrophoresis, the DNA fragments move with different speed to the anode, forming clear bands, which depend on their molecular weights. The results are made visible by means of ethidium bromide or non-toxic dyes like Safe-Red in 302 nm lengths UV light transilluminator. 0.3 % agar gel was prepared by 0.5X TBE buffer containing 0.045M Tris-borate and 0.001M EDTA, which was boiled in microwave at 800 W for 1 min. 2µl Safe-Red was added to every 50 ml gel and the mixture was poured into the gel chamber. Cool down at room temperature and covered the gel by 0.5X TBE buffer. The wells, formed by a gel comb, were filled with the probes which were dyed by DNA loading solution. Exposed to 50 V direct current for 30 min. Then analyzed and documented by AlphaEaseFC software Version 4.0 (Alpha Innotech, CA, USA). Only probes with clear and expected size bands were taken into consideration.

3. 2. 6 Short conventional PCR and mutation control cloning

Mutation controls can originate from cultured cells and sequence-defined mutation specimens. After the genomic DNA templates were amplified by quantitative real time PCR as described above, followed by a short conventional PCR using a gradient Cycler (DNA Engine Thermal Cycler, BIORAD Laboratories, Munich, Germany). 1 µl of PCR products was diluted to a volume of 25µl of PCR mix containing forward and reverse primers (0.1 pmol each), 2 mM dNTPs (Roche), 2 mM $MgCl_2$ (Bioline), 2.55µl Opti Buffer (Bioline), 1µl 0.5µg/µl BSA and 0.5 µl Taq polymerase BIOX-Act Short (Bioline, Luckenwalde, Germany).

Samples were amplified with a pre-cycling hold at 95°C for 2 min, followed by 20 cycles of denaturation at 95°C, annealing at 55°C for 30 sec, elongation at 72°C

for 30 sec, final extension at 72°C for 10 min. Presence of the product was assessed by agarose gel electrophoresis, followed by autoradiographic visualization. Products were obtained by means of Gel Extraction Kit (Qiagen GmbH, Hilden, Germany) following the manufacture's instruction.

The PCR-amplified fragment was cloned into TOPO vector by means of TOPO TA Cloning Kit (Invitrogen, Karlsruhe, Germany), following the manufacturer's instructions. The concentration was assessed by spectrophotometry, ready-to-use mutation control had to be diluted to 1 mg/ml.

3. 3 Statistical analysis

The statistical analysis was performed by SPSS version 20.0 (SPSS Inc., Chicago, IL, USA). The relationship between the *GNAQ* or *GNA11* mutational status and the clinico-pathological parameters, including gender, age, scleral extension, tumor thickness, largest tumor diameter and tumor location was evaluated by Fisher's exact test. The relationship between pathology status and mutational status in *GNAQ* or *GNA11* was evaluated by one-way ANOVA. The correlations between concomitant *GNAQ* and *GNA11* mutations and prognostic features were evaluated by one-way ANOVA. A p-value of less than 0.05 was considered statistically significant.

4. RESULTS

4. 1 Quality of the specimens

In our complete series, only specimens with HMBS c.p-values lower than 39, and showing a detectable melting peak in mutation analysis were considered acceptable for melting curve mutation analysis. Genomic DNA concentrations and quality is illustrated in **Figure 3**. The average concentration was 351.19 (ng/µL), ranging from 12.46 to 2023 (ng/µL), the median of HMBS c.p-value was 34.55, ranging from 22.08 to 38.4

70 (4.2%) out of 1650 cases were excluded in our study due to low DNA quality. The informative rate of our samples was therefore 95.7%.

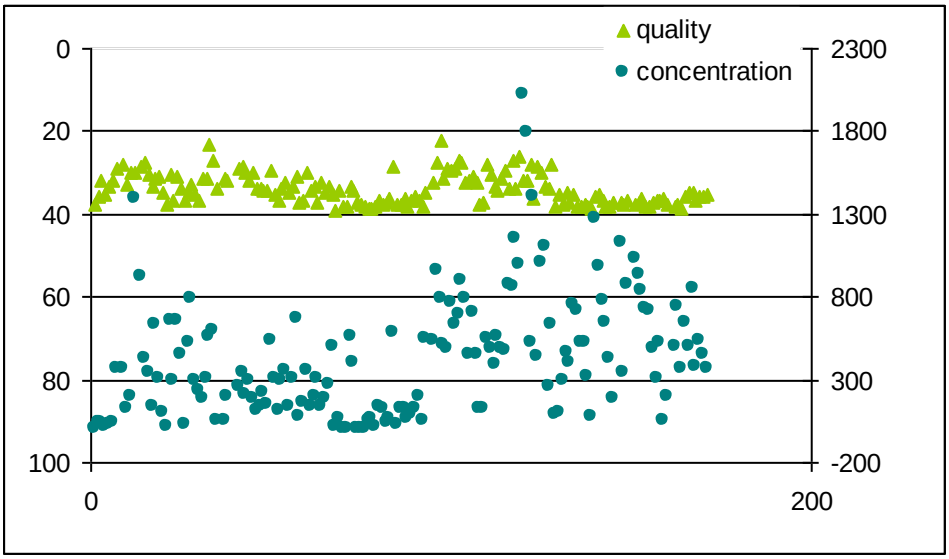

Figure 3. Illustration of genomic DNA concentration and quality

4. 2 Clinico-pathological characteristics

Clinico-pathological characteristics of the patients are summarized in **Table 3**. 165 patients were included in the study. The median age was 57 years, ranging from 22 to 81 years. 68 (41.2%) of the tumors were spindle cell type, 12 (7.3%) epitheloid cell type and 85 (51.5%) mixed cell type. Invasion was found in 107 tumors (64.8%). 145 (87.9%) of primary tumors were larger than 10mm in diameter.

Table 3. Clinico-pathological characteristics of the primary uveal melanomas

Clinico-pathological features	Uveal melanoma
Number of cases, n	165
Median age(range), y	57 (range: 22 to 81)
Gender, n (%)	
Male	87 (52.7)
Female	78 (47.3)
Age, n(%)	
<60	102 (61.8)
≥60	63 (38.2)
Pathology, n(%)	
Spindle	68 (41.2)
Mixed [a]	85 (51.5)
Epithelioid	12 (7.3)
Invasion, n(%)	
yes	107 (64.8)
No	48 (29.1)
Data missing	10 (6.1)
Thickness, n(%)	
≤8.5mm	54 (32.7)
>8.5mm	95 (57.6)
Data missing	16 (9.7)
Diameter, n(%)	
≤10mm	9 (5.5)
>10mm	145 (87.9)
Data missing	11 (6.7)
Location, n(%)	
Anterior	2 (1.2)
Posterior	153 (92.7)
Data missing	10 (6.1)

a combination of epithelioid and spindle cells.

4. 3 Mutational analysis and single strand DNA sequencing

Mutational status was determined by melting curve analysis and sequencing. Figures 4 - 6 are illustrations of PCR employing gDNA from UM specimens and two internal controls (WT and Mut) in optimized quantitative real time PCR to detected mutations in gene GNAQ and GNA11. In gene GNAQ codon 183 (Figure 4), the clear single melting peaks at 60.94°C were generated by mutation specimens and the internal mutation control whereas the melting peaks which produced by wildtype samples were at 66.70°C. Mutations affecting codon 183 in GNAQ were all CGA→CAA (R183Q). In gene GNAQ codon 209 (Figure 5), the clear single melting peaks at 58.26°C were generated by mutation specimens whereas the melting peaks produced by wildtype samples were at 63.16°C. Mutations affecting codon 209 in GNAQ were predominantly CAA→CTA (Q209L). Only one case showed a CAA→CAC transition. In gene GNA11 codon 209 (Figure 6), the clear single melting peaks at 60.23°C were generated by homozygous mutation, CAG→CTG (Q209L). The appearances of a bounce in melting peaks can be explained as heterozygous mutations, which were also defined by single strand DNA sequencing. The melting peaks which produced by wildtype samples were at 66.19°C.

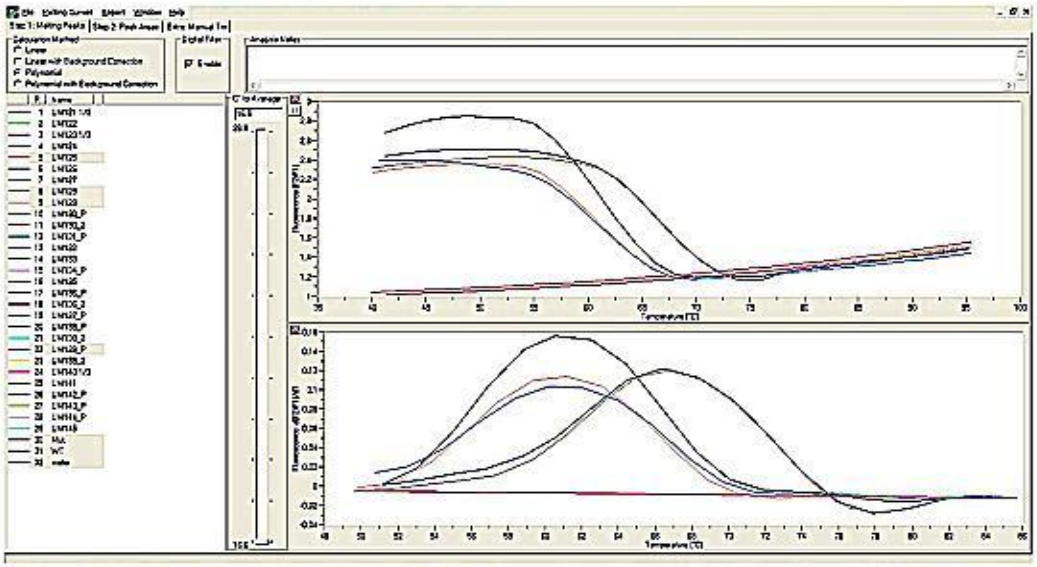

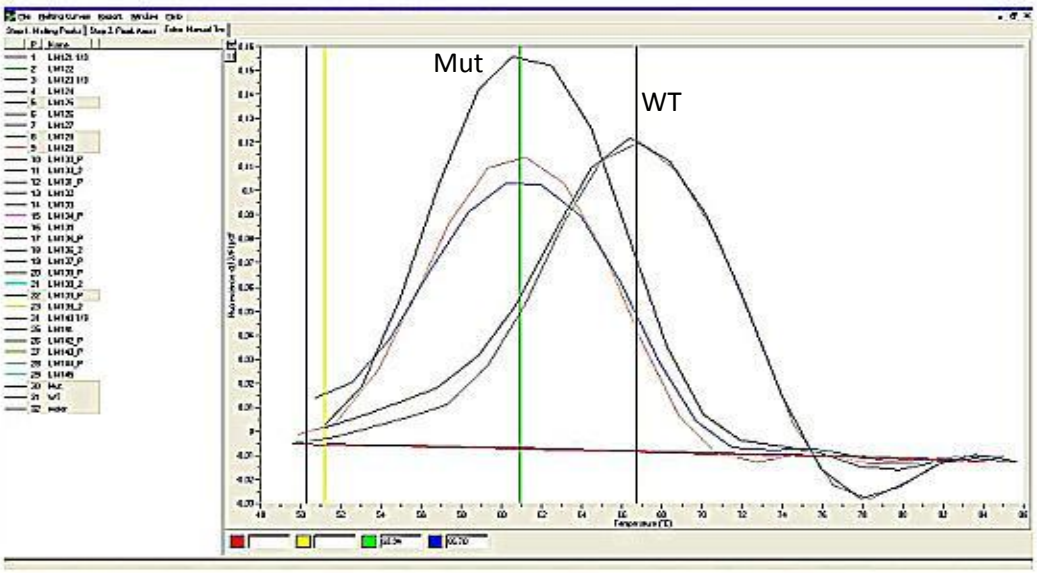

GNAQ-183 cell line 92-1 Fw:
AGCTGGGAAATAGGTTTCATGGACTCAGTTACTACCTGAAAATGACACTTTGTAAGTCAA
AGGGGTATTCGATGATCCCTGTGGTGGGGACTCGAACTCTAAGCACATCTTGTTGCGTAG
GCAGGTAGGCAGGGTCAGCTACGCGGTCCAAGTCATTAAGATAGCTAGAGGAGGGAAGAC
ACAATGAGAATGTCAGTa
Base 93: C (Wildtype)

GNAQ_183 UM Sample #UM60 Fw:
AGCTGGGAAATAGGTTTCATGGACTCAGTTACTACCTGAAAATGACACTTTGTAAGTCAW
AGGGGTATTCGATGATCCCTGTGGTGGGGACTYGAACTCTAAGCACATCTTGTTGCGTAG
GCAGGTAGGCAGGGTCAGCTACGCGGTCCAAGTCATTAAGATAGCTAGAGGAGGGAAGAC
ACAATGAGAATGTCAGTa
Base 60: A+T
Base 93: T+C (Mutated, heterozygote)

GNAQ_183 UM Sample #UM80 Fw:
AGCTGGGAAATAGGTTTCATGGACTCAGTTACTACCTGAAAATGACACTTTGTAAGTCAA
AGGGGTATTCGATGATCCCTGTGGTGGGGACTCGAACTCTAAGCACATCTTGTTGCGTAG
GCAGGTAGGCAGGGTCAGCTACGCGGTCCAAGTCATTAAGATAGCTAGAGGAGGGAAGAC
ACAATGAGAATGTCAGTa
Base 60: A
Base 93: C (Wildtype)

Figure 4. Employing gDNA from UM specimens and internal controls in gene GNAQ 183

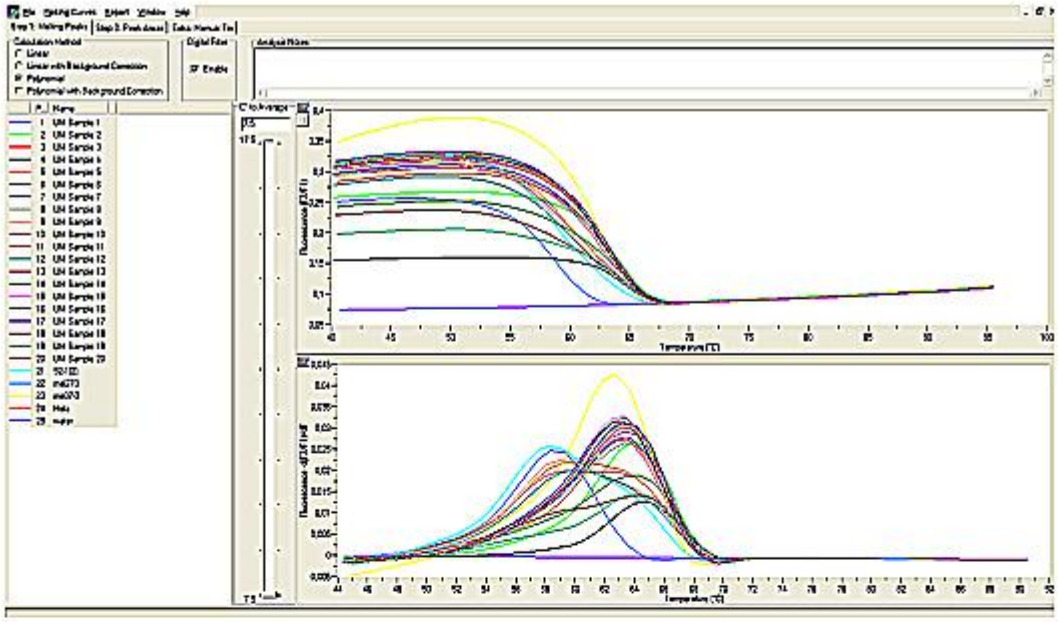

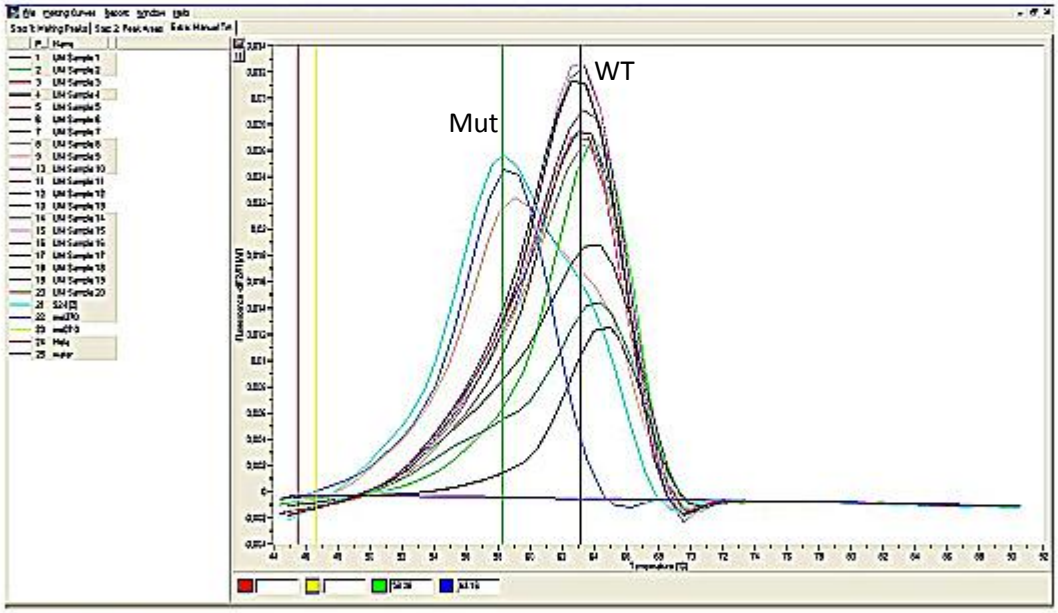

GNAQ-209 cell line Hela Fw:
GAACTTGATCATATTCACTAAGCGCTACTAGAAACATGATAGAGGTGACATTTTCAAAGCAGTGTATCCATT
TTCTTCTCTCTGACCTTTGGCCCCCTACATCGACCATTCTGCAAGGTTAACAATACTCATATTAATAACATA
TAAAGTAAAACTAAAAAGTCAACATAAATATAGCACTACTTACAAACTa
Base 90: T (Wildtype)

GNAQ-209 cell line 92-1 FW:
GAACTTGATCATATTCACTAAGCGCTACTAGAAACATGATAGAGGTGACATTTTCAAAGCAGTGTATCCATT
TTCTTCTCTCTGACCTTwGGCCCCCTACATCGACCATTCTGCAAGGTTAACAATACTCATATTAATAACATA
TAAAGTAAAACTAAAAAGTCAACATAAATATAGCACTACTTACAAACTa
Base 90: A+T (Mutated, heterozygote)

GNAQ_209 UM Sample #UM128 Fw:
GAACTTGATCATATTCACTAAGCGCTACTAGAAACATGATAGAGGTGACATTTTCAAAGCAGTGTATCCATT
TTCTTCTCTCTGACCTGTGGCCCCCTACATCGACCATTCTGCAAGGTTAACAATACTCATATTAATAACATA
TAAAGTAAAACTAAAAAGTCAACATAAATATAGCACTACTTACAAACTa
Base 89: G (Mutated)

Figure 5. Employing gDNA from UM specimens and internal controls in gene GNAQ 209

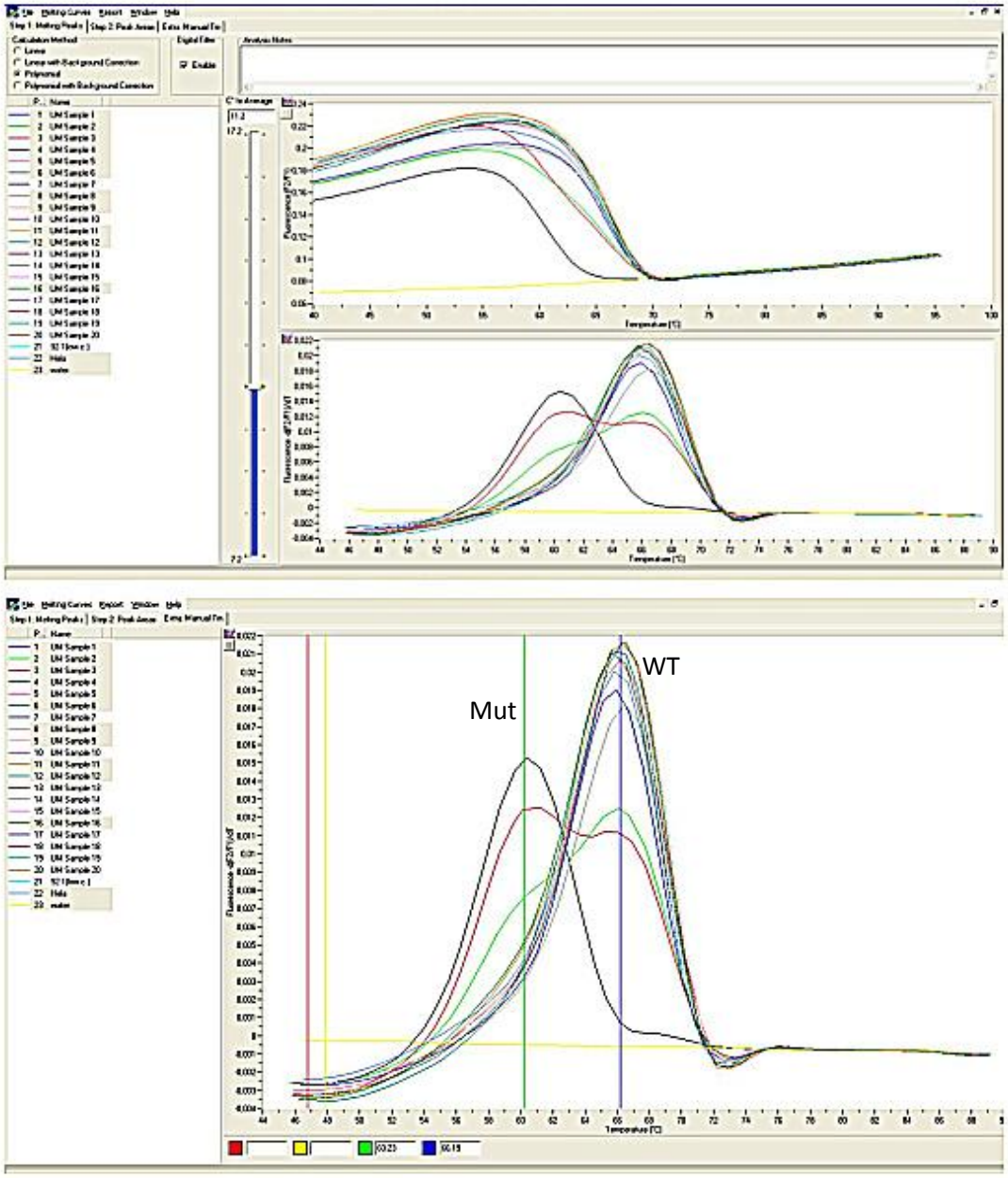

GNA11-209 cell line 92-1 Fw:

GGGAGGGGCTTGGGTGGGAGCCGTCCTGGGATTGCAGATTGGGCCTTGGGGCGCCAGGTGGCTGAGTCCTGG
CGCTGTGTCCTTTCAGGATGGTGGATGTGGGGGGCCAGCGGTCGGAGCGGAGGAAGTGGATCCACTGCTTTG
AGAACGTGACATCCATCATGTTTCTCGTCGCCCTCAGCGAATACGACCAAGTCCTGGTA
Base 109: A (Wildtype)

GNA11-209 UM Sample #UM2 Fw:

GGGAGGGGCTTGGGTGGGAGCCGTCCTGGGATTGCAGATTGGGCCTTGGGGCGCCAGGTGGCTGAGTCCTGG
CGCTGTGTCCTTTCAGGATGGTGGATGTGGGGGGCCWGCGGTCGGAGCGGAGGAAGTGGATCCACTGCTTTG
AGAACGTGACATCCATCATGTTTCTCGTCGCCCTCAGCGAATACGACCAAGTCCTGGTA
Base 109: T+A (Mutated,heterozygote)

GNA11-209 UM Sample #UM4 Fw:

GGGAGGGGCTTGGGTGGGAGCCGTCCTGGGATTGCAGATTGGGCCTTGGGGCGCCAGGTGGCTGAGTCCTGG
CGCTGTGTCCTTTCAGGATGGTGGATGTGGGGGGCCTGCGGTCGGAGCGGAGGAAGTGGATCCACTGCTTTG
AGAACGTGACATCCATCATGTTTCTCGTCGCCCTCAGCGAATACGACCAAGTCCTGGTA
Base 109: T (Mutated)

Figure 6. Employing gDNA from UM specimens and internal controls in gene GNA11 209

Results are summarized in **Tables 4** and **5**.

65.2 % (107/164) of primary UM specimens and 4 out of 6 (66.7%) of UM metastases were mutated in the codon 209 of the gene *GNA11*. Mutations affecting codon 209 in *GNA11* were CAG→CTG (Q209L). One sample harbored a mutation at codon 181 (CGG→CGA). No mutations were found in the codon 183 of *GNA11*.

Mutations at codon 183 of gene *GNAQ* occurred in 24.8% of primary UMs, and in 4 out of 6 (66.7%) specimens of metastatic tissues. Mutations affecting codon 183 in *GNAQ* were all CGA→CAA (R183Q). In the codon 209 of *GNAQ*, 30% of primary UM patients and 1 out of 6 (16.7%) metastasis melanoma patients resulted in mutation. Mutations affecting codon 209 in *GNAQ* were predominantly CAA→CTA (Q209L). Only one case showed a CAA→CAC transition.

One out of 162 (0.6%) primary UM patients and 2 out of 6 (33.3%) cases of metastatic melanomas harbored mutations at codon 603 of *BRAF*. Mutations in the gene *BRAF* were all CGA→CAA (c.1808 G>A; p.R603Q). One of 162 (0.6%) primary UM patients showed a mutation in the codon 12 of the gene *NRAS*, whereas 2/144 (1.3%) of specimens showed mutations in the exon 11 of *KIT* (one located at codon 569 and one at codon 573).

Altogether, 85.5% of primary UM carried mutations in either *GNAQ* or *GNA11* affecting either codon 183 or codon 209 in a predominant pattern, and only 14.5% of primary UM were wild-type for both, *GNAQ* and *GNA11*. Conversely, 26% of primary UMs harbored mutations in both *GNA11* as well as *GNAQ*.

Table 4. Frequency of mutations at codons 183 and 209 of *GNAQ* and *GNA11* in 165 primary uveal melanoma specimens and in 6 matched metastasis tissues

	GNAQ				GNA11				Not GNAQ	
	codon183		codon209		codon183		codon209		or GNA11	
	No.	(%)	No.	(%)	No.	(%)	No.	(%)	No.	(%)
Primary	41/165	24.8	48/160	30.0	0/152	0.0	107/164	65.2	24/165	14.5
Metastasis	4/6	66.7	1/6	16.7	0/6	0.0	4/6	66.7	1/6	16.7

Table 5. Frequency of mutations in BRAF, NRAS, and KIT in 165 primary uveal melanoma specimens and in 6 matched metastasis tissues

	BRAF		NRAS				KIT					
Codon	597-603		12		61		569-573		590		804	
	No.	(%)	No.	(%)	No.	(%)	No.	(%)	No.	(%)	No.	(%)
Primary	1/162	0.6	1/162	0.6	0/152	0.0	2/144	1.3	0/160	0.0	0/159	0.0
Metastasis	2/6	33.3	0/6	0.0	0/6	0.0	0/6	0.0	0/6	0.0	0/6	0.0

4. 4 Correlation between mutation status and clinico-pathological prognostic parameters

We evaluated a possible correlation between *GNAQ* or/and *GNA11* mutational status and clinico-pathological features (**Tables 6 and 7**). Mutations in *GNA11* were found more commonly in primary tumors with thickness > 8.5 mm and diameter > 10 mm and more frequently in specimens with extrascleral extension in comparison to specimens without invasion, but differences were not significant. Concomitant mutations in *GNAQ* and *GNA11* were not significantly associated with any pathological features **(Table 7)**. However, specimens resulted in wild-type for both *GNAQ* and *GNA11* were more frequent in smaller tumors (thickness ≤8.5 mm and diameter ≤ 10 mm) without extrascleral extension compared with tumors with mutation in *GNAQ* and/or *GNA11*.

Table 6. Correlation of GNAQ and GNA11 mutational status of 165 primary uveal melanoma specimens with clinico-pathological characteristics and prognostic indicators

Clinico-pathological feature	$GNAQ^{Mut}$ n (%)	$GNAQ^{WT}$ n (%)	p-value[a]	$GNA11^{Mut}$ n (%)	$GNA11^{WT}$ n (%)	p-value[a]
Gender (n=165)						
Male	40(24.2%)	47(28.5%)	0.6	53(32.1%)	34(20.6%)	0.3
Female	39(23.6%)	39(23.6%)		54(32.7%)	24(14.5%)	
Age, years (n=165)						
<60	50(30.3%)	52(31.5%)	0.7	69(41.8%)	33(20.0%)	0.4
≥60	29(17.6%)	34(20.6%)		38(23.6%)	25(15.2%)	
Pathology (n=165)						
Spindle	30(18.2%)	38(23.0%)	0.3	49(29.7%)	19(11.5%)	0.1
Mixed	44(26.7%)	41(24.9%)		52(31.5%)	33(20.0%)	
Epithelioid	5(3.0%)	7(4.2%)		6(3.6%)	6(3.6%)	
Invasion (n=155)						
yes	49(31.6%)	58(37.4%)	0.7	69(44.5%)	38(24.5%)	0.7
no	24(14.5%)	24(15.5%)		33(21.3%)	15(9.7%)	
Thickness (n=149)						
≤8.5mm	25(16.8%)	29(19.4%)	1.0	33(22.4%)	21(14.1%)	0.5
>8.5mm	45(30.2%)	50(33.6%)		63(42.3%)	32(21.5%)	
Diameter (n=154)						
≤10mm	3(1.9%)	6(3.9%)	0.5	5(3.2%)	4(2.5%)	0.4
>10mm	70(45.5%)	75(48.7%)		96(62.3%)	49(31.8%)	
Location (n=155)						
Anterior	1(0.6%)	1(0.6%)	1.0	1(0.6%)	1(0.6%)	1.0
Posterior	72(46.4%)	81(52.2%)		97(62.5%)	56(36.1%)	

[a] The correlation between patient characteristics and mutational status was determined by Fisher's exact test. A value of $p<0.05$ was regarded as statistically significant.

Table 7. Correlation of GNAQ and GNA11 concomitant mutational status of 165 primary uveal melanoma specimens with clinico-pathological characteristics and prognostic indicators

Prognostic Features	GNAQ/11^{WT}	GNAQ/11^{Mut}	GNAQ^{Mut} or GNA11^{Mut}	p-value
Gender (n=165)				
Male	14(8.5%)	19(11.5%)	54(32.7%)	0.5
Female	11(6.6%)	25(15.2%)	42(25.4%)	
Age, years (n=165)				
<60	14(8.5%)	29(17.6%)	59(35.8%)	0.8
≥60	11(6.6%)	15(9.1%)	37(22.4%)	
Pathology (n=165)				
Spindle	9(5.5%)	20(12.1%)	39(23.6%)	0.7
Mixed	14(8.4%)	23(13.9%)	48(29.1%)	
Epithelioid	2(1.2%)	1(0.6%)	9(5.5%)	
Invasion (n=155)				
yes	16(10.3%)	26(16.8%)	65(41.9%)	0.6
no	7(4.3%)	15(9.7%)	26(16.8%)	
Thickness (n=149)				
≤8.5mm	9(6.0%)	13(8.7%)	32(21.5%)	0.9
>8.5mm	15(10.1%)	26(17.4%)	54(36.2%)	
Diameter (n=154)				
≤10mm	2(1.3%)	1(0.6%)	6(3.9%)	0.9
>10mm	22(14.3%)	41(26.6%)	82(53.2%)	
Location (n=155)				
Anterior	0 (0.0%)	0 (0.0%)	2 (1.3%)	0.2
Posterior	25(16.1%)	39(25.1%)	89(57.4%)	

4. 5 Mutation analysis in primary and matched metastasis specimens

Results are summarized in **Table 8**. Five specimens of primary UM (83%) and 4 out of 6 (67%) of UM metastases were mutated in the codon 209 of the gene *GNA11*. Mutations affecting codon 209 in *GNA11* were CAG→CTG (Q209L). No mutations were identified in the codon 183 of *GNA11*.

Mutations at codon 183 of gene *GNAQ* occurred in 3 (50%) of primary UMs, and in 4 out of 6 (66.7%) specimens of metastatic tissues. Mutations affecting codon 183 in *GNAQ* were all CGA→CAA (R183Q). In the codon 209 of *GNAQ*, only one primary tumor and one metastasis was mutated. Mutations affecting codon 209 in *GNAQ* were all CAA→CTA (Q209L).

BRAF resulted mutated in distant metastases of two patients (33%). Mutations were found at codon 603 of the gene *BRAF* and they were all CGA→CAA (c.1808 G>A; p.R603Q). No mutations were identified in *KIT* or *NRAS*.

Altogether 40 out of 52 mutational statuses matched between primary and metastatic lesions. Five cases of mutation were found in the primary melanoma only and patients #5 and #6 clearly showed mutations only in the primary. Seven cases of mutation were observed only in the metastatic tissue, three of them occurring in the same patient. Patients #2, #3 and #4 showed mutations only in the metastasis. In patient #2 the metastatic tissue displayed mutated *GNA11* codon 209, *GNAQ* codon 209 and *BRAF*, but wild-type at the level of the primary melanoma.

Table 8. Mutational status pattern in 6 matched primary and metastatic uveal melanoma specimens

		GNA11		GNAQ			NRAS		KIT		
Patient	Tissue origin	183	209	183	209	BRAF	12	61	569/572/573	590	804
#1	Primary	WT	Mut	WT	Mut	WT	WT	WT	WT	WT	WT
	Metastasis	WT	Mut	Mut	WT	WT	WT	WT	WT	WT	WT
#2	Primary	WT	WT	Mut	WT	WT	WT	WT	WT	WT	WT
	Metastasis	WT	Mut	Mut	Mut	Mut	WT	WT	ND	WT	WT
#3	Primary	WT	Mut	WT	WT	WT	WT	WT	WT	WT	WT
	Metastasis	WT	Mut	Mut	WT	WT	WT	WT	WT	WT	WT
#4	Primary	WT	Mut	WT	WT	WT	WT	WT	WT	WT	WT
	Metastasis	WT	WT	Mut	WT	Mut	WT	ND	ND	WT	WT
#5	Primary	WT	Mut	Mut	ND	WT	WT	WT	ND	WT	WT
	Metastasis	WT	Mut	WT	WT	WT	WT	WT	WT	WT	WT
#6	Primary	WT	Mut	Mut	ND	WT	WT	ND	ND	WT	WT
	Metastasis	WT	WT	WT	WT	WT	WT	WT	ND	WT	WT

ND: not determined; WT: wild-type form; Mut: mutated form

5. DISCUSSION

In the study we evaluated the presence of mutations in the genes *GNAQ*, *GNA11*, *BRAF*, *NRAS* and *KIT* in primary UM specimens from a large cohort of patients and investigated the association with clinico-pathological prognostic parameters. Furthermore we analyzed the mutational status in six matched primary and metastasis UM specimens to assess for clonal evolution.

5. 1 Frequency of mutations

In our series of samples, more than 80% of primary UMs showed mutations in either *GNAQ* or *GNA11.* Our findings were similar to the results of van Raamsdonk CD et al. [2][3] and confirmed the fact that mutations in the genes *GNAQ* and *GNA11* represent a common and early event in UM development. In comparison to van Raamsdonk in primary UM specimens, we observed a much higher frequency of R183 mutations (24.8% vs. 2.8%) and a relatively low frequency of Q209 mutations (30% vs. 44.8%) in the gene *GNAQ.* Comparison of the frequency is listed below.

Table 9. Summary of published GNAQ and GNA11 mutation studies in ocular melanoma

	GNA11		**GNAQ**	
	R183	**Q209L**	**R183Q**	**Q209L**
Onken MD (2008)	--------	--------	--------	49%(33/67)
van Raamsdonk(2010)	2.1%(3/145)	31.9%(52/163)	2.8%(4/145)	44.8%(73/163)
Pópulo H (2011)	--------	--------	--------	36%(8/22)
In our series	0	65.2%(107/164)	24.8%(41/165)	30%(48/160)

Q209 mutations occurred more often in the primary tumor rather than in the metastasis, whereas in the metastasis, R183 mutations were more common than in the primary tumor. We also observed a higher abundance of mutations at codon 209 in the gene *GNA11* (65.2% vs. 31.9%). *GNA11* mutant tumors may have a higher tendency to metastasize und poorer survival than *GNAQ* mutant tumors. The higher rate of mutation we observed in *GNA11* and in particular at codon 183 of *GNAQ* is consistent with the higher frequency of concomitant mutations we found in our series in comparison to van Raamsdonk's (26 % vs. 0%). A possible explanation for these discrepancies is that our cohort of patients might differ from the cohort of van Raamsdonk's (characteristics of the primary tumor, ethnics, etc), but a comparison could not be performed since the relevant information could not be fully obtained from the reports of van Raamsdonk et al.

Despite the limits imposed by our small series of metastasis samples and by the low frequency of *GNAQ* R183 mutation in the series of van Raamsdonk, the trends were similar in both the series. In additional, the technical errors and carry out contaminations cannot be completely ruled out, although many precautions were taken to exclude technical errors. The higher frequency of R183 mutations in *GNAQ* in the metastasis might suggest a potential role of *GNAQ* mutations at codon 183 in UM progression in respect of Q209 and *GNA11* Q209. However, this is the first report showing a relatively high abundance of R183 mutations in *GNAQ* and a detailed functional characterization of such kind of mutation is still missing.

5. 2 Correlation between mutational status and clinico-pathological prognostic parameters

In line with other reports [2][3][109], we did not observe any significant association between the mutational status of GNAQ, GNA11 or clinico-pathological prognostic parameters, but we found mutations in *GNA11* somewhat more common in primary tumors associated with prognostic adverse features (thickness > 8.5 mm, diameter > 10 mm and scleral invasion). These observations are consistent with the trend also noted by van Raamsdonk et al. [2] and other evidence [110] that suggest that *GNA11* mutations at codon 209 may have a more potent effect on melanocytes than *GNAQ* mutations occurring at the same codon.

Characterization of UM for presence of mutations in *GNAQ* or *GNA11* might identify patients who could benefit from a drug-target based approach. To date, there are no direct inhibitors of *GNAQ* and *GNA11*. However, preclinical data with MEK inhibitors showed efficacy in a *GNAQ*- and *GNA11*-mutant dependent manner [111][112].

It has been extensively documented that MAPK and PI3K/AKT pathways are highly activated in UM [5][110]. The MAPK pathway in cutaneous and mucosal melanoma is usually constitutively activated via *BRAF*, *NRAS* or *KIT*. *BRAF* encodes a serine/threonine kinase downstream for RAS that transduces the regulatory signal through the MAPK pathway. RAS can additional interact with the PI3K pathway leading to apoptosis and cytoskeleton signaling effects. *KIT* encodes a tyrosine kinase whose activation regulates several downstream signal transduction pathways including the MAPK pathway and the PI3K/AKT pathway [73]. In our series of UM, mutations in the genes *BRAF*, *KIT* and *NRAS* were rare, in line with other reports [113][114] supporting the hypothesis that other mechanisms than

activating mutations in *BRAF*, *NRAS* and *KIT* lead to activation of the MAPK and AKT pathway in UM.

5. 3 Clonal evolution of cancer

In our series of samples, 3 specimens showed mutations in *BRAF*. The mutations were all CGA→CAA (c.1808 G>A; p.R603Q) and predominantly in the metastatic tissues (2/6). R603 is located in the activation segment of the kinase domain of *BRAF* and is adjacent to V600, but, since this kind of mutation was not described before and we are not aware whether it leads to an activation of *BRAF*. However, exon 15 mutations not involving the V600 codon are relatively common in melanoma [115][116] and they can be associated with sensitivity to MEK inhibitors [116].

In the analysis of matched primary-metastatic samples, 2 patients (#5 and #6) clearly showed mutations only at the level of the primary tumor. Apart from technical reasons, for example, the presence of stromal tissues that could affect the determination, in order to avoid a false-positive result, these samples were sequenced, so this discrepancy of the mutational status could be explained according to the concept of cancer heterogeneity [117]. The primary tumor might have been heterogeneous in respect of the mutational status of the genes we analyzed and, since we evaluated a single metastasis, a tumour subclone generating that particular metastasis can be postulated.

On the other hand, three patients (#2, #3 and #4) showed mutations only at metastasis. In patient #2 the metastatic tissue showed mutations in three different genes and both patients #2 and #4 harbored the *BRAF* mutation R603Q. These findings could be explained on the basis of to the concept of clonal evolution of cancer, which is linked to the intratumor cellular heterogeneity: selective pressures

allow some mutant subclones to expand and to develop distant metastasis while others become extinct or remain dormant [118]. Clonal evolution of the tumor also represents one of the most important mechanisms of drug resistance in cancer and it is a common cause of target therapy failure.

6. SUMMARY

In summary, our findings showed that mutations in *GNAQ* or *GNA11* are common in primary UM, whereas *BRAF, NRAS* and *KIT* are rare. Genes *GNAQ, GNA11* and *BRAF* are concordant in the majority of cases between primary and metastasis tumors, acquisition of further mutations in these genes can occur during tumor progression.

7. ABBREVIATIONS

°C	Celsius grades
cGy	Centigray
CO2	Carbone dioxide
COMS	Collaborative ocular melanoma study
COX	Cyclooxygenase
c.p-values	Crossing point values
CR	Complete responses
CT	Computed tomography
DMEM	Dulbecco's modified eagle's medium
DMSO	Dimethylsulphoxide
EDTA	Ethylenediaminetetraacetic acid
FBS	Fetal bovine serum
FFA	Fundus fluorescein angiography
FFPE	Formalin fixed paraffin embedded
FNAC	Fine needle aspiration cytology
GDP	Guanosine diphosphate
GTP	Guanosine triphosphate
HMBS	Hydroxymethylbilane synthase
ICGA	Indocyanine green angiography
IHP	solated hepatic perfusion
IO	Indirect ophthalmoscope
MAPK	Mitogen activated protein kinase
mg	Milligram
MgCl2	Magnesium dichloride
min	Minutes
mM	Milli mol
MRI	Magnetic resonance imaging
MSH	Melanocyte-stimulating hormone
mTOR	Mammalian target of rapamycin
Mut	Mutate
NC-Ms	Neural crest-derived melanocytes

OCT	Optical coherence tomography
ODM	Oculodermal melanocytosis
OM	Ocular melanocytosis
PBS	Phosphate buffered saline
PCR	Polymerase chain reaction
PDGFR	Platelet derived growth factor receptors
PFS	Progression free survival
PI3K pathway	Phosphatidylinositol-3-kinase pathway
PLC	Phospholipase C
pmol	Pico mole
PR	Partial responses
PTEN	Phosphatase and tensin homolog
ROS	Reactive oxygen species
RPMI	Roswell park memorial institute
RTK	Receptor tyrosine kinases
SCF	Stem cell factor
SD	Stabilizations of disease
sec	Seconds
TACE	Transarterial chemo embolization
TBE buffer	Tris-Borate-Edta buffer
TSR	Trans-scleral tumor resection
TTT	Transpupillary thermotherapy
UM	Uveal melanoma
UMs	Uveal melanomas
UVB	Ultraviolet B
VEGF	Vascular endothelial growth factor
WT	Wildtype
µl	Microliter

8. REFFERENCES

1. Onken MD, Worley LA, Long MD, et al. Oncogenic mutations in *GNAQ* occur early in uveal melanoma. Invest Ophthalmol Vis Sci. 2008; 49: 5230-4.
2. van Raamsdonk CD, Bezrookove V, Green G, Bauer J, Gaugler L, O'Brien JM, et al. Frequent somatic mutations of *GNAQ* in uveal melanoma and blue naevi. Nature. 2009; 457:599-602.
3. van Raamsdonk CD, Griewank KG, Crosby MB, Garrido MC, Vemula S, Wiesner T, et al. *GNA11* mutations in uveal melanoma. N Engl J Med. 2010; 363:2191-9.
4. Russo AE, Torrisi E, Bevelacqua Y, Perrotta R, Libra M, McCubrey JA, et al. Melanoma: molecular pathogenesis and emerging target therapies (Review). Int J Oncol. 2009; 34:1481-9.
5. Pópulo H, Vinagre J, Lopes JM, Soares P. Analysis of *GNAQ* mutations, proliferation and MAPK pathway activation in uveal melanomas. Br J Ophthalmol. 2011; 95:715-9.
6. Carvajal RD, Antonescu CR, Wolchok JD, Chapman PB, Roman RA, Teitcher J, et al. *KIT* as a therapeutic target in metastatic melanoma. JAMA. 2011; 305:2327-34.
7. Curtin JA, Busam K, Pinkel D, et al. Somatic activation of *KIT* in distinct subtypes of melanoma. J Clin Oncol. 2006; 24: 4340-6.
8. Daniels AB, Abramson DH. c-*KIT* in uveal melanoma: big fish or red herring? Arch Ophthalmol. 2009; 127:695-7.
9. Singh AD, Turell ME, Topham AK. Uveal melanoma: trends in incidence, treatment, and survival. Ophthalmology. 2011; 118:1881-5.
10. Hu DN., Yu GP., Bedikian AY.. Metastatic uveal melanoma therapy: current options. Int Ophthalmol Clin, 2006; 46:151–66.
11. Vajdic CM, Kricker A, Giblin M, et al. Incidence of ocular melanoma in Australia from 1990 to 1998. Int J Cancer. 2003; 105:117-22.
12. Vajdic CM, Kricker A, Giblin M, et al. Eye color and cutaneous mevi predict risk of ocular melanoma in Australia. Int J Cancer. 2001; 92: 906-12.
13. Hu DN, Yu GP, McCormick SA, et al. Population-based incidence of uveal melanoma in various races and ethnic groups. Am J Ophthalmol. 2005a; 140:

612-7.

14. Bergman L, Seregard S, Nilsson B, et al. Incidence of uveal melanoma in Sweden from 1960 to 1998. Invest Ophthalmol Vis Sci. 2002; 43:2579-83.
15. Virgili G, Gatta G, Ciccolallo L, et al. Incidence of uveal melanoma in Europe. Ophthalmology. 2007; 114: 2309-15.
16. Krygier G, Lombardo K, Vargas C, et al. Br J Ophthalmol. 2001; 85: 1007-8.
17. Singh AD, Shields CL, De Potter P, et al. Familial uveal melanoma: clinical observations on 56 patients. Arch Ophthalmol. 1996; 114: 392-9.
18. Canning CR, Hungerford J. Familial uveal melanoma. Br J Ophthalmol. 1988; 72: 241-3.
19. Travis LB, Curtis RE, Boice JD Jr, et al. Second malignant neoplasms among long term survivors of ovarian cancer. Cancer Res. 1996; 56:1564-70.
20. Schoenberg BS, Christine BW. Malignant melanoma associated with breast cancer. South Med J. 1980; 73: 1493-7.
21. Buecher B, Gauthier-Villars M, Desjardins L, et al. Contribution of CDKN2A/P16 (INK4A), P14 (ARF), CDK4 and BRCA1/2 germline mutations in individuals with suspected genetic predisposition to uveal melanoma. Fam Cancer. 2010; 9: 663–7.
22. Abdel-Rahman MH, Pilarski R, Cebulla CM, et al. Germline BAP1 mutation predisposes to uveal melanoma, lung adenocarcinoma, meningioma, and other cancers. J Med Genet. 2011; 48, 856-9.
23. Harbour JW, Onken MD, Roberson ED, et al. Frequent mutation of BAP1 in metastasizing uveal melanomas. Science. 2010; 330:1410-3.
24. Singh AD, Kalyani P, Topham A. Estimating the risk of malignant transformation of a choroidal nevus.Ophthalmology. 2005a; 112: 1784-9.
25. Shields CL, Furuta M, Berman EL, et al. Choroidal nevus transformation into melanoma: Analysis of 2514 Consecutive Cases. Arch Ophthalmol. 2009;127: 981-7.
26. Sumich P, Mitchell P, Wang JJ. Choroidal nevi in a white population: the Blue Mountains Eye Study. Arch Ophthalmol. 1998; 116: 645-50.
27. Ziahosseini K, Mathews D, Biswas S, et al. Idiopathic intracranial hypertension and congenital ocular melanocytosis: a new association. Br J Ophthalmol. 2008; 92: 1430-1.

28. Leung AK, Kao CP, Cho HY, et al. Scleral melanocytosis and oculodermal melanocytosis (nevus of Ota) in Chinese children. J Pediatr 2000; 137: 581-4.
29. Gonder JR, Shields JA, Albert DM, et al. Uveal malignant melanoma associated with ocular and oculodermal melanocytosis. Ophthalmology 1982; 89: 953-60.
30. Shields CL, Shields JA. Ocular melanoma: relatively rare but requiring respect. Clin Dermatol. 2009; 27: 122-33.
31. Muhammad TK, Sanaullah J, Zakir H, et al. Choroidal Melanoma in Ocular Melanocytosis. Pak J Ophthalmol. 2010; 26: 100-3.
32. Kanter-Lewensohn L, Girnita L, Girnita A, et al. Tamoxifen-induced cell death in malignant melanoma cells: possible involvement of the insulin-like growth factor-1 (IGF-1) pathway. Mol Cell Endocrinol. 2000; 165: 131–7.
33. Roberts JE, Wiechmann AF, Hu DN. Melatonin receptors in human uveal melanocytes and melanoma cells. J Pineal Res 2000; 28: 165–71.
34. Lea CS, Holly EA, Hartge P, et al. Reproductive risk factors for cutaneous melanoma in women: a case-control study. Am J Epidemiol. 2007; 165: 505–13.
35. Hartge P, Tucker MA, Shields JA, et al. Case-control study of female hormones and eye melanoma. Cancer Res. 1989; 49: 4622-5.
36. Holly EA, Aston DA, Ahn DK, et al. Uveal melanoma, hormonal and reproductive factors in women. Cancer Res. 1991; 51:1370–2.
37. Behrens T, Kaerlev L, Cree I, et al. Hormonal exposures and the risk of uveal melanoma. Cancer Causes control. 2010; 21:1625-34.
38. Regan S, Judge H E, Gragoudas E S, et al. Iris Color as a Prognostic Factor in Ocular Melanoma. Arch Ophthalmol. 1999; 117: 811-4.
39. Schmidt-Pokrzywniak A, Jöckel KH, Bornfeld N, et al. Positive Interaction Between Light Iris Color and Ultraviolet Radiation in Relation to the Risk of Uveal Melanoma. Ophthalmology. 2009; 116: 340–8.
40. Weis E, Shah CP, Lajous M, et al. The association between host susceptibility factors and uveal melanoma. Arch Ophthalmol. 2006; 124: 54-60.
41. Wakamatsu K, Hu DN, McCormick SA, et al. Characterization of melanin in human iridal and choroidal melanocytes from eyes with various colored irides. Pigment Cell Melanoma Res. 2008; 21: 97-105.
42. Wielgus AR, Sarna T. Melanin in human irides of different color and age of donors. Pigment Cell Res. 2005; 18:454-64.

43. Eagle RC Jr. Iris pigmentation and pigmented lesions: An ultrastructural study. Trans Am Ophthalmol Soc. 1988; 86: 581-687.
44. Rootman J, Gallagher R. Color as a risk factor in iris melanoma. Am J Ophthalmol. 1984; 98: 558-61.
45. Gandini S, Sera F, Cattaruzza MS, et al. Meta-analysis of risk factors for cutaneous melanoma: II. Sun exposure. Eur J Cancer. 2005; 41:45-60.
46. Pleasance ED, Cheetham RK, Stephens PJ, et al. A comprehensive catalogue of somatic mutations from a human cancer genome. Nature. 2010; 463:191-6.
47. Situm M, Buljan M, Bulic SO, et al. The mechanisms of UV radiation in the development of malignant melanoma. Coll Antropol. 2007; 31:13-6.
48. Kurzel R, Wolbarsht ML, Yamanashi BS. Ultraviolet radiation effects on the human eye. Photochem. Photobiol. 1977; 2: 133-67.
49. Boettner EA, Walter JR. Transmission of the ocular media. Invest Ophthalmol Vis Sci. 1962; 1: 776-83.
50. Singh AD, Rennie IG, Seregard S, et al. Sunlight exposure and pathogenesis of uveal melanoma. Surv Ophthalmol. 2004; 49: 419-28.
51. Shields JA, Shields SC. (1992) Intraocular tumor: A text and atlas. Saunders WB, Philadelphia, p. 54-306.
52. Hu DN. Photobiology of ocular melanocytes and melanoma. Photochem Photobiol. 2005b; 81: 506-9.
53. Singh AD, Bergman L, Seregard S. Uveal melanoma: epidemiologic aspects. Ophthalmol Clin North Am. 2005b; 18: 75-84.
54. Yu GP, Hu DN, McCormick SA. Latitude and incidence of ocular melanoma. Photochem Photobiol. 2006; 82:1621-6.
55. Hu DN, Simon JD, Sarna T. Role of ocular melanin in ophthalmic physiology and pathology. Photochem Photobiol. 2008; 84: 639-44.
56. Herlyn M, Nathanson KL. Taking the guesswork out of uveal melanoma. N Engl J Med. 2010; 363: 2256-7.
57. Lamba S, Felicioni L, Buttitta F, et al. Mutational profile of *GNAQ*Q209 in human tumors. PLoS One. 2009; 4: e6833.
58. Bauer J, Kilic E, Vaarwater J, et al. Oncogenic *GNAQ* mutations are not correlated with disease-free survival in uveal melanoma. Br J Cancer. 2009; 101: 813-5.

59. Dhomen N, Marais R, *BRAF* Signaling and Targeted Therapies in Melanoma. Hematol Oncol Clin North Am. 2009; 23: 529-45.
60. Fensterle J. A trip through the signaling pathways of melanoma. Ein Streifzug durch die (Signal-)Wege des malignen Melanoms. J Dtsch Dermatol Ges. 2006; 4: pp. 205-17.
61. Davies H, Bignell GR, Cox C, et al. Mutations of the *BRAF* gene in human cancer. Nature. 2002; 4: 949-54.
62. Zuidervaart W, van Nieuwpoort F, Stark M, et al. Activation of the MAPK pathway is a common event in uveal melanomas although it rarely occurs through mutation of *BRAF* or RAS. Br J Cancer. 2005; 92: 2032-8.
63. Calipel A, Mouriaux F, Glotin AL, et al. Extracellular signal-regulated kinase-dependent proliferation is mediated through the protein kinase A/B-Raf pathway in human uveal melanoma cells. J Biol Chem. 2006; 281: 9238-50.
64. Weber A, Hengge UR, Urbanik D, et al. Absence of mutations of the *BRAF* gene and constitutive activation of extracellular regulated kinase in malignant melanomas of the uvea. Lab Invest. 2003; 83: 1771-6.
65. Stahl JM, Sharma A, Cheung M, et al. Deregulated Akt3 activity promotes development of malignant melanoma. Cancer Res. 2004; 64: 7002-10.
66. Stahl JM, Cheung M, Sharma A, et al. Loss of PTEN promotes tumor development in malignant melanoma. Cancer Research. 2003; 63: 2881–90.
67. Robertson GP. Functional and therapeutic significance of Akt deregulation in malignant melanoma. Cancer and Metastasis Reviews. 2005; 24: 273-85.
68. Ehlers JP, Worley L, Onken MD, et al. Integrative genomic analysis of aneuploidy in uveal melanoma. Clin Cancer Res. 2008; 14: 115-22.
69. Ibrahim N, Haluska FG. Molecular pathogenesis of cutaneous melanocytic neoplasms. Annu Rev Pathol. 2009; 4: 551-79.
70. Mouriaux F, Kherrouche Z, Maurage CA, et al. Expression of the c-kit receptor in choroidal melanomas. Melanoma Res. 2003; 13: 161-6.
71. Antonescu CR, Busam KJ, Francone TD, et al. L576P *KIT* mutation in anal melanomas correlates with *KIT* protein expression and is sensitive to specific kinase inhibition. Int J Cancer. 2007; 121: 257-64.
72. Beadling C, Jacobson-Dunlop E, Hodi FS, et al. *KIT* gene mutations and copy number in melanoma subtypes. Clin Cancer Res. 2008; 14: 6821-8.

73. Willmore-Payne C, Holden JA, Tripp S, et al. Human malignant melanoma: detection of BRAF- and c-kit-activating mutations by high-resolution amplicon melting analysis. Hum Pathol. 2005; 36: 486-93.
74. Wallander ML, Layfield LJ, Emerson LL, et al. *KIT* mutations in ocular melanoma: frequency and anatomic distribution. Mod Pathol. 2011; 24: 1031-5.
75. Klintworth GK, Scroggs MW: The eye and ocular adnexa. In: Sternberg SS, ed.: Diagnostic Surgical Pathology. Philadelphia, Pa: Lippincott Williams & Wilkins, 1999, pp. 994-6.
76. Bedikian AY. Metastatic uveal melanoma therapy: current options. Int Ophthalmol Clin. 2006; 46: 151-66.
77. Diener-West M, Reynolds SM, Agugliaro DJ, et al. Screening for metastasis from choroidal melanoma: the Collaborative Ocular Melanoma Study Group Report 23. J Clin Oncol. 2004; 22: 2438-44.
78. Shields JA, Shields CL. Prognostic factors for uveal melanoma. Gospodarowicz M, O'Sullivan B, Sobin LH.Prognostic Factors in Cancer. 3rd ed Hoboken, NJ Wiley-Liss Inc. 2006; 269-72.
79. Shields JA, Shields CL. Intraocular Tumors: An Atlas and Textbook. 2nd ed. Philadelphia, PA Lippincott Williams & Wilkins. 2008; 85-175.
80. Damato B, Duke C, Coupland SE, et al. Cytogenetics of uveal melanoma: A 7-year clinical experience. Ophthalmology. 2007; 114: 1925-31.
81. Kujala E, Mäkitie T, Kivelä T. Very long-term prognosis of patients with malignant uveal melanoma. Invest Ophthalmol Vis Sci. 2003; 44: 4651-9.
82. Damato B, Eleuteri A, Fisher AC, et al. Artificial neural networks estimating survival probability after treatment of choroidal melanoma. Ophthalmology. 2008; 115: 1598-607.
83. Harbour JW. Molecular prognostic testing and individualized patient care in uveal melanoma. Am J Ophthalmol. 2009; 148: 823-9.
84. Kilic E, Naus NC, van Gils W, et al. Concurrent loss of chromosome arm 1p and chromosome 3 predicts a decreased disease-free survival in uveal melanoma patients. Invest Ophthalmol Vis Sci. 2005; 46: 2253-7.
85. Hausler T, Stang A, Anastassiou G, et al. Loss of herterozygosity of 1p in uveal melanomas with monosomy 3. Int J Cancer. 2005; 116: 909-13.
86. van den Bosch T, van Beek JG, Vaarwater J, et al. Higher percentage of FISH-

determined monosomy 3 and 8q amplification in uveal melanoma cells relate to poor patient prognosis. Invest Ophthalmol Vis Sci. 2012; 53: 2668-74.

87. Singh AD, Topham A. Survival rates with uvealmelanoma in the United States: 1973-1997. Ophthalmology. 2003; 110: 962-5.
88. Jensen OA. Malignant melanomas of the human uvea: 25-year follow-up of cases in Denmark, 1943-1952. Acta Ophthalmol. (Copenh) 1982; 60: 161-82.
89. Raivio I. Uveal melanoma in Finland. An epidemiological, clinical, histological and prognostic study. Acta Ophthalmol. Suppl 1977; 133: 1-64.
90. Diener-West M, Reynolds SM, Agugliaro DJ, et al. Development of metastatic disease after enrollment in the COMS trials for treatment of choroidal melanoma. Collaborative Ocular Melanoma Study Group Report No. 26. Arch Ophthalmol. 2005; 123: 1639-4.
91. Damato B, Dopierala JA, Coupland SE. Genotypic profiling of 452 choroidal melanomas with multiplex ligation-dependent probe amplification. Clin Cancer Res. 2010;16: 6083-92.
92. Orcurto V, Denys A, Voelter V, et al. (18)F-fluorodeoxyglucose positron emission tomography/computed tomography and magnetic resonance imaging in patients with liver metastases from uveal melanoma: results from a pilot study. Melanoma Res. 2012; 22: 63-9.
93. Servois V, Mariani P, Malhaire C, et al. Preoperative staging of liver metastases from uveal melanoma by magnetic resonance imaging (MRI) and fluorodeoxyglucose-positron emission tomography (FDG-PET). Eur J Surg Oncol. 2010; 36:189-94.
94. Bechrakis NE, Petousis V, Krause L, et al. Surgical treatment modalities in uveal melanomas. Klin Monbl Augenheilkd. 2009; 226: 921-6.
95. Diener-West M, Earle JD, Fine SL, et al. The COMS randomized trial of iodine 125 brachytherapy for choroidal melanoma, III: initial mortality findings. COMS Report No. 18. Arch Ophthalmol. 2001; 119: 969-82.
96. Lommatzsch PK, Werschnik C, Schuster E. Long-term follow-up of Ru-106/Rh-106 brachytherapy for posterior uveal melanoma. Graefes Arch Clin Exp Ophthalmol. 2000; 238: 129-37.
97. Finger PT, Chin KJ, Duvall G. Palladium-103 ophthalmic plaque radiation therapy for choroidal melanoma: 400 treated patients. Ophthalmology. 2009;

116: 790-6.

98. Becker JC, Terheyden P, Kämpgen E, et al. Treatment of disseminated ocular melanoma with sequential fotemustine, interferon alpha, and interleukin 2. Br J Cancer. 2002; 87: 840-5.

99. Peters S, Voelter V, Zografos L, et al. Intra-arterial hepatic fotemustine for the treatment of liver metastases from uveal melanoma: experience in 101 patients. Ann Oncol. 2006; 17: 578-83.

100. Sato T, Eschelman DJ, Gonsalves CF, et al. Immunoembolization of malignant liver tumors, including uveal melanoma, using granulocyte-macrophage colony-stimulating factor. J Clin Oncol. 2008; 26: 5436-42.

101. Yamamoto A, Chervoneva I, Sullivan KL, et al. High-dose immunoembolization: survival benefit in patients with hepatic metastases from uveal melanoma. Radiology. 2009; 252: 290-8.

102. Penel N, Delcambre C, Durando X, et al. O-Mel-Inib: a Cancero-pole Nord-Ouest multicenter phase II trial of high-dose imatinib mesylate in metastatic uveal melanoma. Investig New Drugs. 2008; 26: 561–5.

103. Hofmann UB, Kauczok-Vetter CS, Houben R, et al. Overexpression of the *KIT*/SCF in uveal melanoma does not translate into clinical efficacy of imatinib mesylate. Clin Cancer Res. 2009; 15: 324–9.

104. Marshall JC, Fernandes BF, Di Cesare S, et al. The use of a cyclooxygenase-2 inhibitor (Nepafenac) in an ocular and metastatic animal model of uveal melanoma. Carcinogenesis. 2007; 28: 2053-8.

105. Kabbinavar FF, Hambleton J, Mass RD, et al. Combined analysis of efficacy: the addition of bevacizumab to fluorouracil/leucovorin improves survival for patients with metastatic colorectal cancer. J Clin Oncol. 2005; 23: 3706-12.

106. Sandler A, Gray R, Perry MC, et al. Paclitaxel-carboplatin alone or with bevacizumab for non-small-cell lung cancer. N Engl J Med. 2006; 355: 2542-50.

107. Oku T, Tjuvajev JG, Miyagawa T, et al. Tumor growth modulation by sense and antisense vascular endothelial growth factor gene expression: effects on angiogenesis, vascular permeability, blood volume, blood flow, fluorodeoxyglucose uptake, and proliferation of human melanoma intracerebral xenografts. Cancer Res. 1998; 58: 4185-92.

108. Chan KR, Gundala S, Laudadio M, et al. A pilot study using sunitinib malate

as therapy in patients with stage IV uveal melanoma. J Clin Oncol. 2008; 26: (abstract)

109. Daniels AB, Lee JE, Macconaill LE, et al. High throughput mass spectrometry-based mutation profiling of primary uveal melanoma. Invest Ophthalmol Vis Sci. 2012; 53:6991-6.

110. Takasaki J, Saito T, Taniguchi M, et al. A novel Galphaq/11-selective inhibitor. J Biol Chem. 2004; 279:47438-45.

111. Khalili JS, Yu X, Wang J, Hayes BC, Davies MA, Lizee G, et al. Combination small molecule MEK and PI3K inhibition enhances uveal melanoma cell death in a mutant *GNAQ*- and GA11-dependent manner. Clin Cancer Res. 2012; 18:4345-55.

112. Ho AL, Musi E, Ambrosini G, Nair JS, Deraje NVasudeva S, de Stanchina E, et al. Impact of combined mTOR and MEK inhibition in uveal melanoma Is driven by tumor genotype. PLoS One 2012; 7: e40439.

113. Cruz F 3rd, Rubin BP, Wilson D, Town A, Schroeder A, Haley A, et al. Absence of *BRAF* and *NRAS* mutations in uveal melanoma. Cancer Res. 2003; 63: 5761-6.

114. Platz A, Egyhazi S, Ringborg U, Hansson J.. Human cutaneous melanoma; a review of *NRAS* and *BRAF* mutation frequencies in relation to histogenetic subclass and body site. Mol Oncol. 2008; 1: 395-405.

115. Beadling C, Heinrich MC, Warrick A, et al. Multiplex mutation screening by mass spectrometry evaluation of 820 cases from a personalized cancer medicine registry. J Mol Diagn. 2011; 13: 504-13.

116. Dahlman KB, Xia J, Hutchinson K, et al. *BRAF* L597 mutations in melanoma are associated with sensitivity to MEK inhibitors. Cancer Discov. 2012; 2:791-7.

117. Marusyk A, Almendro V, Polyak K. Intra-tumour heterogeneity: a looking glass for cancer? Nat Rev Cancer. 2012; 12: 323-34.

118. Greaves M, Maley CC. Clonal evolution in cancer. Nature. 2012; 481:306-13.

9. CURRICULUM VITAE

19.08.2013

Signature:

10. ACKNOWLEDGEMENTS

I would like to cordially to thank the following persons and institutions, without whom this work and my presence in Berlin would have been impossible.

Prof. Dr. med. Ulrich Keilholz

Dr. Alberto Fusi

Dr. med. Gergor Willerding

Prof. Dr. med. Antonia Joussen

Aline Isabel Riechardt

Anika Nonnenmacher

Alexander Gross

The colleagues from the Department of Hematology and Medical Oncology of Charité-CBF

The colleagues from the Department of Ophthalmology of Charité-CBF

My family, for their love and support

My friends

11. ZUSAMMENFASSUNG

Das Aderhautmelanom ist der häufigste intraokulare Tumor, mit einer starken Neigung zur Metastasierung. Das Vorkommen von extraokulärem Wachstum, Rezidiven oder Metastasen ist mit einer schlechteren Prognose assoziiert. Aktuell gibt es keine Standard-Behandlung für das metastasierte uveale Melanom. Die Genotypisierung von UMs könnte eine Identifizierung von Patienten ermöglichen, die von einer zielgerichteten Therapie profitieren könnten.

Die vorliegende Studie untersucht den *GNAQ*, *GNA11*, *BRAF*, *NRAS* und *KIT* Mutationsstatus und die Assoziation klinisch-prognostischer Parameter in einer großen Serie von Aderhautmelanomen. Zur Beurteilung der klonalen Evolution wurde bei 6 Patienten zudem das Metastasengewebe analysiert. Unsere Ergebnisse zeigten, dass Mutationen in *GNAQ* oder *GNA11* in primäre UM häufig sind, während *BRAF*, *NRAS* und *KIT* selten sind. Die Gene *GNAQ*, *GNA11* und *BRAF* stimmen in der Mehrzahl der Fälle zwischen Primarius und Metastase überein, aber während der Tumorprogression können zusätzliche Mutationen in diesen Genen auftreten.

12. AFFIDAVIT

I, Yuehua Mai certify under penalty of perjury by my own signature that I have submitted the thesis on the topic [Mutation Analysis in Uveal Melanoma: Evidence for Clonal Evolution]. I wrote this thesis independently and without assistance from third parties, I used no other aids than the listed sources and resources.

All points based literally or in spirit on publications or presentations of other authors are, as such, in proper citations indicated. The sections on methodology and results correspond to the URM (uniform requirements for manuscripts) and are answered by me. My interest in any publications to this dissertation corresponds to those that are specified in the following joint declaration with the responsible person and supervisor. All publications resulting from this thesis and which I am author correspond to the URM and I am solely responsible.

The importance of this affidavit and the criminal consequences of a false affidavit are known to me and I understand the rights and responsibilities stated therein.

Date: 19. 08. 2013. Signature: